

NUMERICAL ANALYSIS OF MAGNETOHYDRODYNAMIC  
EFFECT AND WALL SLIP FOR NON NEWTONIAN FLUID FLOW  
IN MICROCHANNELS

Thesis submitted by  
Satyabrata Podder

Doctor of Philosophy (Engineering)

Department of Mechanical Engineering  
Faculty Council of Engineering & Technology  
Jadavpur University  
Kolkata, India  
2022

**JADAVPUR UNIVERSITY  
KOLKATA 700032, INDIA**

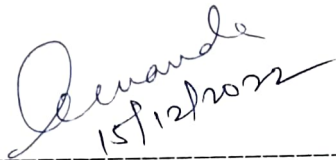
INDEX NO. 182/15/E

1. Title of the thesis:  
NUMERICAL ANALYSIS OF MAGNETOHYDRODYNAMIC EFFECT AND WALL SLIP FOR NON-NEWTONIAN FLUID FLOW IN MICROCHANNELS
2. Name, Designation & Institution of the Supervisor:  
Dr. Arunabha Chanda  
Professor, Department of Mechanical Engineering  
Jadavpur University  
Kolkata- 700032
3. List of Publication:
  - i. Satyabrata Podder, Paulam Deep Paul and Arunabha Chanda, “ The effect of the magnetic field of high intensities on velocity profiles of slip driven non-Newtonian fluid flow through the circular, straight microchannel”, International Journal of Engineering Trends and Technology, Volume 70, Issue 4, pp. 383-388, April, 2022.
  - ii. Satyabrata Podder, Paulam Deep Paul and Arunabha Chanda, “Magnetohydrodynamics (MHD) induced slip flow of a non-Newtonian fluid through circular microchannels”, Trends in Sciences, Volume 19, No. 19, October, 2022.
4. List of Patents: Nil
5. List of Presentations in National/ International/ Conferences/ Workshops:
  - i. Satyabrata Podder and Arunabha Chanda, “Slip flow of non-Newtonian fluids through circular microchannels”, Proceedings of the 25th National and 3rd International ISHMT-ASTFE Heat and Mass Transfer Conference (IHMTTC-2019), December 28-31, 2019, IIT Roorkee, Roorkee, India.
  - ii. Satyabrata Podder, Susobhan Misra and Arunabha Chanda, “Analysis of magnetohydrodynamic slip flow of non-Newtonian fluids through circular microchannels” Proceedings of the 8th International and 47th National Conference on Fluid Mechanics and Fluid Power (FMFP), December 09-11, 2020, IIT Guwahati, Assam, India.

JADAVPUR UNIVERSITY  
FACULTY OF ENGINEERING AND TECHNOLOGY  
DEPARTMENT OF MECHANICAL ENGINEERING  
KOLKATA, INDIA

CERTIFICATE FROM THE SUPERVISOR

This is to certify that the thesis entitled “NUMERICAL ANALYSIS OF MAGNETOHYDRODYNAMIC EFFECT AND WALL SLIP FOR NON-NEWTONIAN FLUID FLOW IN MICROCHANNELS” submitted by Shri Satyabrata Podder, who got his name registered on 18/12/2015 for the award of Ph. D. (Engineering) degree of Jadavpur University is absolutely based upon his own work under the supervision of Dr. Arunabha Chanda and that neither his thesis nor any part of the thesis has been submitted for any degree/ diploma or any other academic award anywhere before.



-----

Dr. Arunabha Chanda

Signature of the Supervisor  
and date with Office Seal

*Professor*  
*Dept. of Mechanical Engineering*  
*Jadavpur University, Kolkata-32*

## “Statement of Originality”

I Satyabrata Podder registered on 18/12/2015 do hereby declare that this thesis entitled “NUMERICAL ANALYSIS OF MAGNETOHYDRODYNAMIC EFFECT AND WALL SLIP FOR NON-NEWTONIAN FLUID FLOW IN MICROCHANNELS” contains literature survey and original research work done by the undersigned candidate as part of Doctoral studies.

All information in this thesis have been obtained and presented in accordance with existing academic rules and ethical conduct. I declare that, as required by these rules and conduct, I have fully cited and referred all materials and results that are not original to this work.

I also declare that I have checked this thesis as per the “Policy on Anti Plagiarism, Jadavpur University, 2019”, and the level of similarity as checked by iThenticate software is 8%.

Signature of Candidate:



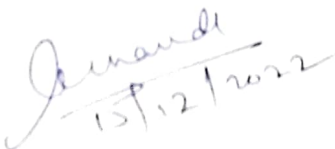
Date:

15/12/2022

Certified by Supervisor:

(Signature with date,

seal)



15/12/2022  
Professor  
Dept. of Mechanical Engineering  
Jadavpur University, Kolkata-32

1. Dr. Arunabha Chanda

## Acknowledgement

At the very outset, I would sincerely like to acknowledge the generous and arduous assistance and inspiration provided by my honorable supervisor Professor Dr. Arunabha Chanda, Mechanical Engineering Department, Jadavpur University. It will not be exaggerated to mention that without their novel ideas, intellectual support, encouragement and enthusiasm, this research could not have reached this stage. I have cherished, learnt and enriched myself from every moment of interaction with him in course of preparation of this thesis.

I would also like to express my deepest regards to Prof. (Dr.) Amit Karmakar, Head, Mechanical Engineering Department, Jadavpur University for his encouragement and support. I humbly acknowledge the generous support of all former head of the departments - Prof. Dipankar Sanyal, Prof. Sankar Dhar, Prof. Goutam Majumdar and Prof. Sumanta Neogi.

I pay sincere thanks to my parents, for their endless supports. My accomplishments and success are because of them only. I also thank my wife and daughter for their selfless support.

I also sincerely acknowledge the management of Supreme Knowledge Foundation Group of Institutions, Mankundu, for providing me the necessary leaves to carry out this research.

 15/12/2022

---

Satyabrata Podder

## Contents

	Page no.
List of Publications and Presentations from the Thesis	i
Certificate from the Supervisor	ii
Statement of Originality	iii
Acknowledgement	iv
Contents	v-vii
List of Symbols	viii
List of Figures	ix-x
List of Tables	xi
Abstract	xii
<b>CHAPTER 01: INTRODUCTION</b>	<b>1-9</b>
1.1 Slip flow in microchannels and microdevices	2
1.2 Characterization of slip flow for liquids	4
1.3 Magnetohydrodynamics induced slip flow through microchannels	6
1.4 Different engineering applications of magnetohydrodynamics induced slip flow through microchannels for advanced materials	8
<b>CHAPTER 02: LITERATURE REVIEW</b>	<b>10-33</b>
2.1 Slip flow in different engineering applications	10
2.2 Slip flow in microchannels	13
2.3 Applications of magnetohydrodynamics (MHD) in slip flow	21
2.4 Applications of MHD induced slip flow for modern fluids for engineering applications	27
2.5 Scope and objective of the present work	32
<b>CHAPTER 03: MATHEMATICAL ANALYSIS AND NUMERICAL SIMULATION</b>	<b>34-46</b>
3.1 Mathematical analysis of slip flow of non-Newtonian fluids	34
3.1.1 Problem statement	37
3.2 Mathematical analysis of magnetohydrodynamics	38
3.2.1 Physical considerations used for MHD induced slip flow	40
3.2.2 Fluid properties	40

3.3 Dimensionless parameters	41
3.4 Numerical simulation	42
3.4.1 Validity and accuracy	43
3.4.2 Stability and convergence	43
3.5 Mesh independence test	44
<b>CHAPTER 04: RESULTS AND DISCUSSION</b>	<b>47-62</b>
4.1 Slip flow of non-Newtonian fluids through circular microchannels	47
4.1.1 Validation slip flow of non-Newtonian fluids	47
4.1.2 Results of slip driven flow of non-Newtonian fluids through microchannels	49
4.2 Results and discussion of slip flow of Xanthan solution in formic acid	55
4.2.1 Validation of a conducting fluid under the influence of externally applied magnetic field	55
4.2.2 Results of slip flow of Xanthan solution in formic acid	56
<b>5.0 CONCLUSIONS</b>	<b>63-64</b>
5.1 Slip flow of non-Newtonian fluids through microchannels	63
5.2 Slip flow of Xanthan solution through microchannel under the influence of externally applied magnetic field	63
5.3 Future scope of work	64
<b>Appendix</b>	<b>65-66</b>
A.1 Data sheet showing the results of numerical analysis of 0.5wt/vol% Xanthan solution in formic acid	65
A.2 Data sheet showing the results of numerical analysis of 1.0 wt/vol% Xanthan solution in formic acid	65
A.3 Data sheet showing the results of numerical analysis of 1.5wt/vol% Xanthan solution in formic acid	66
<b>References</b>	<b>67-75</b>

## LIST OF SYMBOLS

$B_0$	Externally applied magnetic field (T)
$D$	Diameter
$f$	Friction factor, dimensionless
$Ha$	Hartmann No., dimensionless
$k$	Consistency index, $\text{kg S}^{(n-2)}/\text{m}$
$l$	Length of the microchannel
$L$	Length of the microchannel, dimensionless
$n$	Flow behavior index, dimensionless
$P$	Pressure (Pa)
$r$	Radial coordinate, (m)
$R_0$	Radius of circular microchannel (m)
$Re$	Reynolds number, dimensionless
$R$	Radius of the microchannel, dimensionless
$u$	Axial velocity (m/s)
$v$	Velocity (m/s)
$V$	Velocity, dimensionless
$z$	Axial coordinate (m)
<b>Greek symbols</b>	
$\beta$	Slip coefficient, dimensionless ( $= \frac{v_s}{v_m}$ )
$\gamma$	Shear rate ( $\text{s}^{-1}$ )
$\eta$	Apparent viscosity ( $\text{Pa} \cdot \text{s}$ )
$\mu$	Viscosity ( $\text{Pa} \cdot \text{s}$ )
$\rho$	Density ( $\text{kg}/\text{m}^3$ )
$\sigma$	Electrical conductivity ( $(\Omega\text{m})^{-1}$ )
$\tau$	Shear stress ( $\text{N}/\text{m}^2$ )
<b>Subscripts</b>	
$e$	At entrance region
$h$	Hydraulic quantity
$\text{max}$	Maximum value
$m$	Average value
$r$	Along $r$ direction
$s$	Slip value



## List of Figures

Figure No.	Description	Page No.
01	Schematic representation of slip flow	3
02	Direction of externally applied magnetic field ( $B_0$ ) and Lorentz force	7
03	Electromagnetic pumping	7
04	Circular microchannel showing cylindrical co-ordinates	34
05	Flow through a circular channel	35
06	Computational domain of the slip flow in circular microchannel	38
07	Schematic diagram of the flow field under the effect of externally applied Magnetic field	38
08	Comparison of velocity profiles obtained from three different mesh resolutions for $n=0.5$ and $\beta=0.2$	44
09	Comparison of velocity profiles obtained from three different mesh resolutions for $n=1.0$ and $\beta=0.2$	45
10	Comparison of velocity profiles obtained from three different mesh resolutions for $n=1.25$ and $\beta=0.2$	45
11	Generated mesh showing finer distribution of mesh towards wall and centerline	46
12	Comparison of velocity profiles obtained in present work and previous studies	48
13	Velocity profiles of slip flow through microchannel for different flow behaviour index	49
14	Velocity profiles of slip flow through microchannel for different slip co-efficient	50
15	Relation between slip length and slip coefficient.	51
16	Comparison of developed maximum velocity ( $V_{max}$ ) and Slip Coefficients ( $\beta$ )	51
17	Effect of hydraulic diameter ( $D_h$ ) on Poiseuille No. ( $C_f Re$ )	52

## List of Figures

Figure No.	Description	Page No.
18	Effect of slip coefficients on Poiseuille No.	52
19	Effect of slip length ( $l_s$ ) on $C_f$ , $Re$ values	53
20	Effect of Reynold's No. on $C_f$ , $Re$ values	54
21	Sample diagram of the distribution of velocity in the flow field	55
22	Comparison of centreline velocity ( $v_{max}$ ) obtained in present work and previous studies	56
23	Comparison of velocity profiles of slip and no slip flows for different values of slip co-efficient ( $\beta$ ) when no magnetic field is applied	57
24	Comparison of velocity profiles for different values of applied magnetic field ( $B_0$ ) when slip co-efficient ( $\beta$ ) is 0.2	57
25	Comparison of velocity profiles for the different values of $\beta$ when applied magnetic field ( $B_0$ ) is held constant to 0.3T	58
26	Effect of Hartmann No ( $Ha$ ) on $V_{max}$	58
27	Effect of Hartmann No ( $Ha$ ) on $V_{slip}$	59
28	Effect of Hartmann No ( $Ha$ ) on Slip co-efficient ( $\beta$ )	60
29	Comparison of $V_{max}$ v/s $X$ for $B_0=0.4T$ for the different values of $\beta$	60
30	Comparison of $f.Re$ v/s $X$ for $B_0=0.4T$ for the different values of $\beta$	61
31	Velocity profiles of Xanthan solutions of different concentrations	62

## List of Tables

Table No.	Description	Page No.
01	Properties of Xanthan solution in formic acid (25 °C)	41
02	Result for Mesh Independence Study for $\beta=0.2$	44
03	Centerline velocities ( $V_{\max}$ ) obtained for slip and no-slip conditions	48
04	f.Re values obtained from present work and previous studies for slip and no-slip conditions	48
05	Comparison of the developed $V_{\max}$ for different MHD	61
06	Comparison of the developed $V_{\text{slip}}$ for different MHD	62

## Abstract

The flow of non-Newtonian fluids through microchannels often shows slip velocity near microchannel walls. This can be seen for hydrodynamic, fully developed, steady, laminar flow of pseudoplastic and dilatant fluids. A numerical analysis is done for fully developed, steady laminar flow of non-Newtonian fluids by the help of power law model. Governing equations were analysed and applied in the numerical analysis along with slip boundary condition at walls. Circular cross section of the microchannel is considered for analysis. Velocity fields along with other slip flow parameters like slip co-efficient, slip length, friction factor have been compared for pseudoplastic and dilatant fluids.

Further, this analysis is extended by considering the flow of a non-Newtonian fluids having electrical conductivity through circular microchannel which is under the influence of externally applied magnetic field. For the purpose, fluid properties of Xanthan solution in formic acid were considered for the analysis. Velocity fields containing slip velocity and centreline velocities were observed under the influence of magnetic field which was in the range of 0.1 T to 0.4 T. The effects of slip co-efficient and magnetic fields were observed. The influence of Hartmann number was also observed on the slip velocities and centreline velocities. A comparison of friction factor has been done along the length of the microchannel to understand the effect of slip co-efficient on the magnetohydrodynamics (MHD) induced slip flow.

# INTRODUCTION

---

In the last few decades, rapid and prominent development of a new range of devices is observed. These devices have completely different length scale than that of conventional ones. Scientists and researchers have worked together to find out the behaviour and characteristics of various devices when their dimensions are brought down to micrometres. It has been keenly observed that in microscale, the performance of the devices change. Most of the time these changes have proven to be advantageous in the field of fluid flow, mass and heat transfer, biological fluid analysis, drug delivery etc. This new scope of development was discovered by many researchers and consequently a whole new range of devices have evolved in today's world. These devices are known as microelectromechanical systems (MEMS).

As the name implies MEMS distinctively have two major areas of sub grouping. The first one is micro mechanical system and the second one is micro electrical and microelectronic systems. In the mechanical components of MEMS micro sized pumps, heat sinks, heat exchangers, gyroscopes, accelerometers, etc. have become popular [1]. Micro sized pumps, heat sinks, heat exchangers etc. uses various networks of microchannels which controls the fluid flow through microchannels using flow channels, sensors, valves, pumps etc.

'Microchannel' is a channel (square, rectangular or circular) which is used in Microelectromechanical (MEMS) system for certain advantages like faster analysis and response times due to short diffusion distances and other associated factors like compactness, low fabrication cost etc. For a circular microchannel the size may vary on the basis of the fluid it handles. Various experiments show that for liquids hydraulic diameter ( $d_h$ ) is measured between 200  $\mu\text{m}$  and 1000  $\mu\text{m}$  and for gases hydraulic diameter ( $d_h$ ) is found between 10  $\mu\text{m}$  and 200  $\mu\text{m}$ . The concept of microchannel was first reported by Tuckerman and Pease in 1981. Here in this context it should be noted that, for gases flowing through conventional channels the minimum channel dimension is more than 3mm.

For any liquid to flow through the microchannels, most of the application can be seen in the field of bio fluids. Blood, the most popular example of bio fluids and some other bio fluids like DNA,

proteins, enzymes etc. are popularly being analyzed using microdevices. Most of the bio fluids exhibit the nature of non-Newtonian fluid flow. Power law model can be used [2] to describe this type of fluid flow when they are exposed to microchannels. To describe the fluid flow characteristics of these types of bio fluids and other fluids power law indices like flow behavior index ( $n$ ) and consistency index ( $K$ ) have become important [3]. In present days to understand fluid behavior in fluid machineries, numerical simulation is done. In fluid mechanics computational fluid mechanics (CFD) lays the foundation of the numerical simulation which leads to the results showing the possibility of having a practical solution to a complex physical problem [4] [5]. As the success of numerical simulation there is a prominent development of micro flows and microfluidics which predicts the possibility of physical flow situations in a correct manner. This advantageous application of CFD in the field of microfluidics leads to a successful research arena not only in present days but also in the future days to come.

### **1.1 Slip flow in microchannels and microdevices**

With the advent of microdevices, the study of flow characteristics through microchannels has become a popular area of research. It is observed that when fluids pass through microchannels the nature of flow behavior changes due to the reduced length scales from the conventional values to micro level. One of the major behavioral changes can be noted as slip flow which is not a common phenomenon in traditional fluid flow through channels of various cross sections. This drifting into no-slip to slip regime in the flow through microchannels makes the research a challenging one. The fluid layer at the vicinity of the microchannel walls do not stick with the solid wall because of the increased value of surface to volume of the fluid. Instead of sticking on solid walls which is very common in no slip condition in conventional fluid mechanics, for slip flow the fluid layer at the vicinity of the microchannel walls attains a velocity, which is commonly known as slip velocity ( $v_s$ ). Therefore, like macroscopic length scales, no slip boundary condition is no longer applicable for microchannels. Instead, slip boundary condition is applied in microchannels flows. The concept of slip flow and slip boundary condition was formulated by Navier in 1823. In slip boundary model slip velocity ( $v_s$ ) is proportional to the local shear rate at the wall ( $\gamma_{wall}$ ). Here  $l_s$  can be termed as proportionality constant which is known as slip length. Slip length, as shown in Fig.01 can be explained as the linearly

extrapolated velocity profile from the wall surface to the length that would corresponds to no slip boundary condition. Therefore, Navier's slip velocity can be written as:  $v_s = l_s \times \gamma_{wall}$

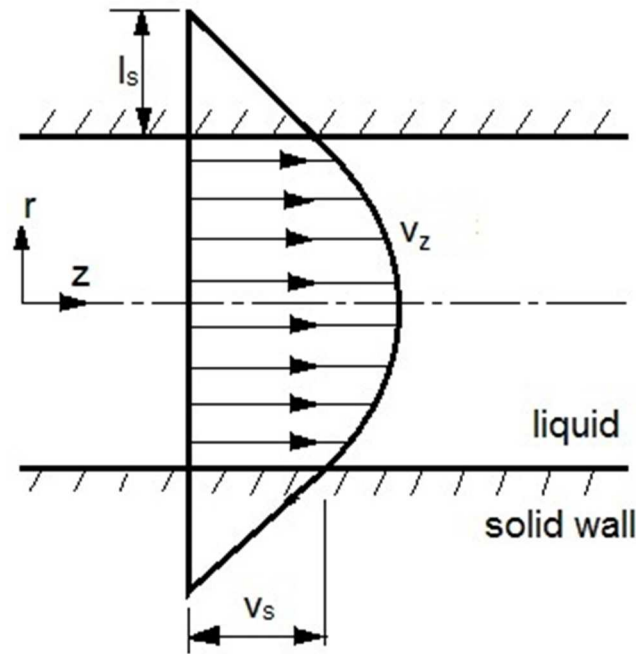


Fig. 01 Schematic representation of slip flow

Slip velocity is caused by many reasons which are now being explored by researchers and scientists. One of the primary reasons behind the slippage at the wall is shear rates. There remains a certain value of critical shear [6] upon which the possibility of slip depends. For the values of low shear rate, no-slip condition is applicable. Although when the shear rate crosses the value of critical shear, slip occurs at the vicinity of the wall. For gaseous flow, in slip regime, there remains a thin gas film in between the wall and the fluid [7]. Molecular simulation shows that the nature of wall also has prominent influence on the fluid to have slip flow on the wall [8]. For example, hydrophobic wall reduces solid-liquid friction which play a roll behind the slip velocity. There are other parameters like thermometric diffusivity or mass density which affects the extent of slip velocity in the micro channel [9]. As the research develops different expressions have been developed for gases and liquids separately. In molecular dynamics the equation of slip velocity can be expressed using Van der Waals forces [10]. Slip is observed in molecular simulation also. In molecular to micro level, slip can be described using local surface

inclination and local film thickness. Geometric parameters like hydraulic diameter are one of few parameters which affect the possibility of slip flow for both gases and liquids [11].

There are various methods available to analyze the physical problem like slip flow. Both analytical and numerical methods [12] are being applied to explore the nature and characteristics of slip flow. Microchannels that handle biofluids can be analyzed using power law model. Numerical analysis of power law fluids through microchannels [13] shows viscous effects and surface effects dominates the flow which also causes non-Newtonian fluids to slip on solid wall. Since slip flow is a boundary phenomenon, slip velocity can be incorporated in the governing equation as boundary condition. Which can be further be classified as first order boundary condition and second order slip boundary condition [14]. Biofluids like blood [15] can be well described as non-Newtonian fluids which points to the possible huge application area in days to come.

A Newtonian fluid's viscosity remains constant irrespective of the amount of shear application for a constant temperature however Non-Newtonian fluids are where the viscosity decreases or increases depending on the fluid. Bio fluids (drugs, blood, protein etc.) show non Newtonian flow behavior when passed through microchannel. Most of the research works describe non Newtonian Fluids with the help of Ostwald de-Waele model. In present days, the fluid flow of non-Newtonian fluids with slip boundary condition is an interesting area of research which lays foundation of many devices and instruments in MEMS.

## **1.2 Characterization of slip flow for liquids**

Apart from the gaseous flow, modern research works have revealed that slip flow may happen in liquids also. The slip phenomenon is proven to be a very common in microchannels which handles biofluids. To explore the nature of these kinds of flows numerical methods have proven to be a useful one [16]. Numerical works require proper boundary condition to be applied in the flow modelling for better simulation. In most of the early works, shear rate near the wall is identified as one of the major causes of slip flow [17]. To find the root causes, the molecular dynamics (MD) theory is employed. Solid wall properties like surface corrugation and wall density have been identified as major influential parameters that causes slip flow. Microscale flow differs from macroscopic for two reasons. Firstly, small scale makes molecular effects such as wall slip and secondly, amplification of magnitudes of velocity, discharge of flow to higher



levels. Here most significant observation in flow through microchannel is slip flow. As per MD theory, possibility of occurrence of slip depends upon surface energy corrugation. This is the potential energy distribution on surface of the channel wall. When a liquid atom is moving forward on channel wall, it would feel corrugation because of mutual interactions of liquid atoms. In molecular dynamics, this is known as atomic stick slip which indicates an effective height. This effective height is a barrier which is caused by the potential energy of the channel walls. An atom is required to overcome this barrier to slip on a surface to move forward along the direction of the velocity of the fluid flow. The extent of slip depends upon the nature of the flow (whether it is hydrophobic or hydrophilic) on the nature of the surface of the channel walls (whether it is hydrophobic or hydrophilic) at micro scale. The degree of slip can be described by a general boundary condition proposed by Navier, in which velocity at the solid wall or in other words slip velocity is proportional to the local shear rate.

The expression of general boundary conditions shows that slip length is also an important parameter along with the slip velocity [18]. Interfacial parameters like wall fluid coupling, surface energy are also few reasons which are proven to be causes of slip flow. The presence of slip also affects the value of entrance length [19]. Experimental works reveal that traditional fluid mechanics equations derived from Navier Stokes equation can be applied in microchannels [20] with proper boundary conditions. With the help of the traditional fluid mechanics knowledge, commercially available software packages are now being used for slip flow simulations through microchannels. The nature of wall, whether it is hydrophilic or hydrophobic also affects the velocity near channel walls and slip length [21]. For hydrophobic wall apparent slip velocity appears. This happens due to the presence of apparent viscosity near wall. This apparent viscosity is different than that of bulk viscosity [22]. The apparent slip velocity and apparent viscosity destabilizes the flow. On contrary sleep flow always stabilizes the flow. Besides numerical and experimental methods, analytical methods are also being employed to model slip flow [23] for different geometries through microchannels. Newtonian fluids have viscosity which remains constant throughout the variation of shear application for a constant value of temperature. However for non-Newtonian fluids a change in viscosity can be observed. When the electrostatic charges are considered electro viscosity appears under consideration [24]. The various aspects of viscosity are explored for non-Newtonian fluids when they pass through microchannels. When nanofluids are mixed in non-Newtonian fluids then the flow behaviour

study becomes an interesting area of research [25]. Slip flow also an inherent characteristics of these types of fluid flow. In these types of fluid flow, the study of velocity profiles and heat transfer characteristics become popular [26]. Entropy generation of non-Newtonian slip flow for different micro geometrics proves the possibility of different engineering applications [27] [28]. As the slip flow is noted as a near wall phenomenon, wall friction properties along with the friction factor, Poiseuille no and viscoelasticity are usually taken into the consideration [29] [30]. Various analytical techniques like homotopy perturbation method [31], boundary element method [32] etc. is applied along with the numerical [33] and experimental methods [34]. Slip flow characterization for nanofluids in microchannels is also under consideration to explore a better understanding [35]. Input parameters like geometry [36], pressure [37], and hydraulic diameter are also under the close observation which may improve slip flow. Numerical works show the effects of various dimensionless numbers and power law indices on the slip flow of non-Newtonian fluids through microchannels [38] [39] [40]. Various applications with different cross sections [41] [42] is explored which provides us a better understanding of slip induced flow of non-Newtonian fluids through microchannels. Heat transfer characteristics [43] along with the experimental validation [44] give us about the fluid flow and mass transfer results [45] [46]. Non Newtonian fluids leading to nonlinear differential equations are solved [47] to understand heat transfer [48], entropy generation [49] and above all fluid flow characteristics with the help of dimensionless numbers for the biofluids in which most of the common example is blood [50].

### **1.3 Magnetohydrodynamics induced slip flow through microchannels**

Magnetohydrodynamics (MHD) is the study of the results of applied magnetic fields on moving fields which are conductor in nature. The study of MHD confined itself into the mutual interaction between moving fluid field and magnetic field. Here the fluid must be electrically conducting in nature. MHD can be applied in engineering applications like pumping, melting, stirring [51] etc.

The flow in fluid field and the coupling of magnetic field with fluid flow can be understood by the electric current ( $J$ ) induction due to the flow of conducting fluid through an externally applied magnetic field ( $B_0$ ). By the interaction between electric current and magnetic field, Lorentz force is generated in the flow field of electrically conducting materials. This is shown in

Fig. 02, in which the situation of magnetic induction is shown schematically for a micro-tube of length 'L'.

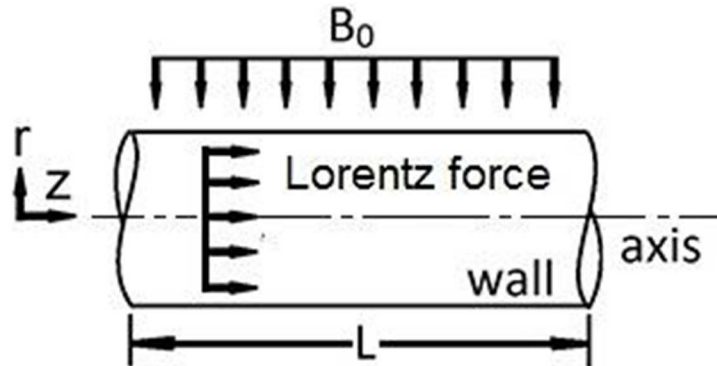


Fig. 02 Direction of externally applied magnetic field ( $B_0$ ) and Lorentz force

This physical phenomenon can be understood if we refer Fig. 03. The principle of electromagnetic pumping is depicted schematically in which the direction of electric flow ( $J$ ) and magnetic field ( $B$ ) is shown. By the interaction of  $J$  and  $B$ , the Lorentz force ( $J \times B$ ) is acting along the flow of the conducting fluids through a channel of circular cross section.

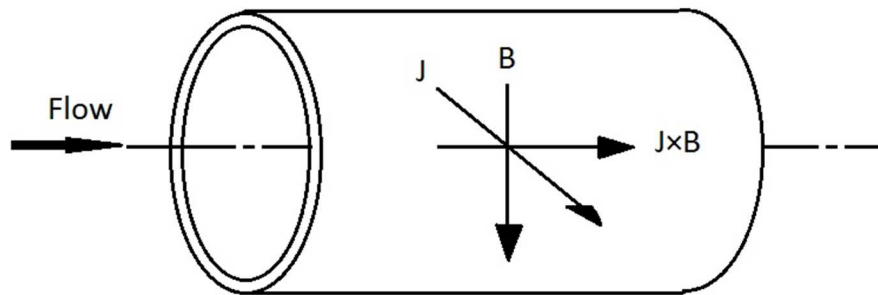


Fig. 03 Electromagnetic pumping

Presently the knowledge of MHD is being applied in microdevices [52] also. In modern researches numerical methods [53] are being applied to analyze the nature of flow through microchannels. When MHD is applied in materials then a dimensionless number, Hartmann no ( $Ha$ ) is used [54] to understand the effect of MHD on fluid flow. Numerical works validated with experimental results shows us the effect of MHD [55] on fluid flow through microchannels. The intensity of applied MHD can be varied from fractions to as high as 10 to 15 Tesla [56]. The

study of fluid field along with the heat transfer values [57] is now an interesting area of research [58] [59]. Numerical analysis focuses in the area of fluid flow and heat transfer [60] for various geometrics [61] to understand the fluid flow in engineering applications like micro pump. To incorporate the effect of slip flow [62] various wall properties and duct geometrics [63] are now being considered. The knowledge of MHD effects on conducting fluids through microdevices is now being applied in various engineering applications like Jeffrey fluids [64], inclined geometrics [65], lid driven cavity [66] or in the application of porous media [67] [71]., stretching surfaces [68] or lid driven cavity applications [69] reveals the effect of MHD on ferrofluids. Biofluids like blood is now being taken into the area of research of magnetohydrodynamics. Peristaltic waves [70] along with slip flow of non-Newtonian biofluids are now an emerging area of research. Hartmann no ranging from few fraction to 5 Tesla is being applied on blood to observe its nature of flow through microchannels and porous media [71]. Along with flow characteristics, heat transfer performance [72], [73] are also being assessed with a special reference of nanoparticle [74], suspended with the flow field. Wall properties like waviness are being taken into consideration in terms of sinusoidal roughness. Results show that an attention is required in this field of research to know the velocity distribution for slip induced flow of non-Newtonian fluids which are under the influence of non-Newtonian fluids. Slip coefficient ( $\beta$ ), slip length ( $l_s$ ) and the effect of MHD on these parameters [75] is still required to be explored with more attention. Slip velocity ( $v_s$ ), f. Re values at the vicinity of the wall is under the effect of Ha, power law index (n) and consistency index (K) for MHD induced slip flow of non-Newtonian fluids has got an enormous possibility of research work in recent days. The modeling of blood through porous media [77] and microchannels [78] is now a prime area of research which requires more attention to understand the effect of applied magnetic fields on electrically conducting fluids.

#### **1.4 Different engineering applications of magnetohydrodynamics induced slip flow through microchannels for advanced materials**

The principle of MHD actuation was first observed by William Ritchie in 1832. This principle was applied on electromagnetic pump. But in last century the development of this research area was not observed in greater extent until the works of J. Hartmann was published in 1918. In the early 1960s the application of MHD started its exploration in the area of engineering in greater

extent. The early examples of the applications of MHD are on liquid metals [79]. Modern engineering applications include nanofluids filled enclosure [80] and channels [81] of various geometrics and cross sections [82]. Alumina [83] [88] [89] and copper [93] [94] [95] [96] nanoparticles mixed with water are now being used to analyze the effect of MHD on conducting fluids through microchannels. Findings of the effect of power law indices [84] on the slip flow of non-Newtonian fluids [85] reveals the fluid flow characteristics in microdevices. Now blood is also being modeled as nanoparticles carrying conducting media [86] to analyze the effect of antibiotics and antibacterial activities. Commercial CFD packages have demonstrated their capabilities to be used in the analysis [87] of these types of fluids. Study of viscosity, shear rate, slip velocity, slip length etc. is now being done of alumina nanofluids [90], silver nanoparticles [91] or ferrous nanoparticles [92]. Presently researchers explored few advantageous features of MHD like heat transfer enhancement [97], for hybrid nanofluid flow [98]. In nanoparticles mixed fluids the viscosity [98] and other fluid properties changes in such a fashion which is causing the development of the advantageous applications of MHD in microchannels. The rheological properties with power law indices [100] also play an important role behind the successful application of MHD in microdevices. Not only in inorganic polymeric fluids has this same tendency also extended its stretch into the biofluids like proteins [100], blood [101] and polysaccharides [102].

## LITERATURE REVIEW

---

In this section relevant works of slip flow through microchannels with emphasis on non-Newtonian fluids which is under influence of externally applied magnetic field is detailed with the work carried out on various fluid characteristics like input parameters, velocity, pressure, wall friction, shear stress, shear rate, slip coefficient.

All of these, in one way or another, helped in advancement of the knowledge in the relevant and concerned fields, to understand the state of the art, identify research gaps, and to determine the scope of work, including the target, and to plan how to address to that.

### 2.1 Slip Flow in Different Engineering Applications

Slip flow is a deviation from the traditional no slip flow. This type of flow can be observed in microdevices which uses the networks of microchannels. A series of work has been done on the primary observation of the nature and characteristics of slip flow. The deviation from the no slip to slip regime is now a known physical phenomenon which is established by the works accomplished by various researchers and scientists. Following are few works mentioned here. These works are referred in connection of the present work for the literature review.

**Gad-el-Hak [1]** in 1999 demonstrated the range of the characteristics length of electro mechanical devices in micro order, the length scale of micro devices in MEMS was explained. This work also demonstrates the viability of using microdevices for magnetic and electrostatic applications. This work showed how dimensionless members and the governing equations of fluid mechanics modelling are affected by length scales of micro order. Liquid flow boundary conditions for micro devices have been discussed in there. This work notes a relationship between slip flow and dimensionless parameters to provide a range of slip possibilities for liquid flows through microchannels.

**Bird et.al. [2]** in 1987 outlined the kinetic theory and fluid mechanics of polymeric liquids. The governing equations and their solutions for diverse engineering applications are adequately explained with the help of boundary conditions. Here, different characteristics of Newtonian and

non-Newtonian fluid flow are illustrated using the usual no slip equation. It is well discussed how to represent non-Newtonian fluids by moving from constitutive equations to special equations appropriate for a certain application.

**Chhabra and Richardson [3]** in 2008 showed the applications of non-Newtonian flow in engineering applications. The rheology of non-Newtonian fluids is explained. The behaviour of non-Newtonian fluids in micro level is explained also. The flow of non-Newtonian fluids pertaining from no-slip flow is analysed with the help of power law model. The liquid phase and multi-phase non-Newtonian fluid flow is explained with ease.

**Anderson [4]** in 1995 classified the scope and application of numerical procedure and techniques in computation fluid mechanics and fluid dynamics as well. The discretization of governing equations after non-dimensionalisation is explained and various numerical techniques along with their application is described.

**Patankar [5]** in 1980 presented advanced algorithms and techniques to solve computational fluid demands. Numerical methods have been discussed for different fluid mechanics applications with a broad survey. Various discretization schemes and techniques are discussed and illustrated examples of liquid flows are depicted.

**Brochard and De Gennes [6]** in 1992 addressed fluid flow mechanisms for a polymer near solid surfaces. Expressions of critical values for shear stress and shear rate were obtained after taking into account shear dependent flow in order to establish polymer chain slippage close to the wall. With rising shear stress levels, a shift from a no slip to a slip regime was seen. To comprehend the change between no slip flow regimes, the wall interactions and friction parameters were also examined.

**P.G. de Gennes [7]** in 2002 explained some non-polymeric fluids' flow behaviour, which showed incredibly low friction against solid walls. They based their reasoning on the idea that there is a very thin gaseous layer between the fluid and the solid wall. They discovered that if the film thickness  $h$  is very thin, the fluctuation of Navier length  $b$  is quite high and independent of the thickness of the gaseous layer. The study also stressed that only a tiny amount of gas is necessary to lubricate the interface between a liquid and a solid, and it came to the conclusion that a liquid that has been oversaturated with gas may be to blame for the remarkably high Navier length.

**Bocquet and Barrat [8]** in 2007 discussed the flow near solid interfaces at different scales from nano to micro in connection with the development of micro fluid devices. The heat transport across interfaces and the effect of surface slip on electro-osmotic flows was also explained in their study.

**Brenner Howard [9]** in 2012 offered a macroscopic approach of the solution to slip flow problem by imposing slip boundary condition on the fluid velocity at a solid boundary in tangential direction. He constituted a rational equation of slip-velocity which a simple fluid faces at it's boundary with a solid wall.

**Pismen and Rubinstein [10]** in 2001 analysed slip conditions in terms of kinetic theory. Macroscopic factors like contact angles, particle density, temperature etc. have been analysed to find out their effect on the microscopic observations like slip length, slip velocity and slip coefficient. This work also considers Van-der Waals forces to find out the expression of dynamic contact angles.

**Hetsroni, Msyak, Pogrebnyak and Yarin [11]** in 2005 contrasted the results from conventional theory to the experimental data on fluid flow in microchannels of various shapes and sizes. They discovered that the experimental results and the theoretical one agreed fairly well. They continued making analogies between liquid and gas. Additionally, they discovered that the relationship between hydraulic diameter and microchannel length and the Reynolds number strongly influence how viscous energy dissipates on flow parameters.

**Heseinzadeh, Heyns, Chamkha and Shir Khanai [12]** in 2019 investigated the transfer of heat through porous fin enclosure and compared the analytical methods with numerical one to validate the solutions. They also investigated the effects of different parameters like porosity ( $S_n$ ), convection ( $N_c$ ), Rayleigh number ( $R_a$ ) on heat transfer as well as the deriving process of the temperature gradient along the fin length.

**Sarabandi and Moghadam [13]** analysed the non-Newtonian laminar flow with the help of power-law model in circular micro-channel imposing a uniform and constant thermal flux. They investigated the variation of entropy generation with the Brickman number and the floe behaviour index.

**Avramanko, Dmitrenko and Shevchuk [14]** in 2020 examined the second-order boundary conditions for the incompressible steady-state fluid flow and heat transfer in a micro-confusor. Based on their research, they were able to derive certain analytical answers for the Nusselt



number, friction coefficient, and velocity and temperature profiles. The study's findings led to the conclusion that as Knudsen number increases, Nusselt number decreases, indicating little interaction between flowing fluid and the surface. Additionally, it was discovered that the second order boundary condition affects the velocity profile of flow but not the characteristics of heat transfer, only the fluctuation of friction coefficient.

**Chakraborty [15]** in 2005 devised a mathematical tool to analyze flow of blood droplets into a micro-fluidic channel and also studied the role of RBC particulates on flow characteristics (non-Newtonian), estimated role of hydraulic resistance in slip flow regimes and also effect of contact angles on slip flow. This study may be benefitted for the precise design of different biomedical devices and helpful in progression of numerous biotechnological applications.

## **2.2 Slip Flow in Microchannels.**

With the development of new concept of slip flow and slip phenomenon in microchannels, the possibility of the application in various engineering applications, have opened a whole new area of research. Following are the works which have been studied to understand the extent of the applications of slip flow in various types of microchannel for Newtonian and non-Newtonian fluids. The summarized form of a vast theoretical development have been observed in following works which are generally focused upon the various parameters and analysis of different flow characteristics that may affect the flow. A change dimensionless numbers or operating input parameters like pressure or in some cases a change in geometry or cross-section have been done to discover various aspects of slip flow in microchannels.

**Crochet and Walters [16]** in 1983 had done numerical simulation on Non-Newtonian flow of liquids (high elastic) in complex geometrics. Different constitutive model had been employed for the consideration of dependent variable. Finite element and finite difference techniques had been applied to differential and integral constitutive models.

**Thompson and Robbins [17]** in 1990 studied the shear flow and structure of LJ fluids near solid boundaries. They showed the wide variation of structure and slip-lengths ( $L_s$ ) of fluids with the wall fluid interaction strength and the wall geometry. They also established the correlation between the changes in flow boundary conditions and the changes in degree of order induced in fluid flow.

**Thompson and Troian [18]** in 1957 worked on a general boundary condition when the fluid flows on a solid wall. The developed boundary condition in general form is able to describe no slip boundary condition as well as slip boundary condition. Based on molecular dynamics a simulation model is proposed for steady state fluid flow for the expression of velocity near solid wall. The slip phenomenon is explained in terms of slip-length, surface energy corrugation, wall fluid coupling and wall density. It is also noted that the shear rate and slip length are two main factors that controls slip flow at the solid boundary of a microchannel.

**Ameel, Wang, Barron, Warrington,Jr. [19]** in 1997 presented an analytical model of gas flow in circular micro tubes with heat flux and slip boundary conditions at wall. This work solved the problem using an indirect method which involves a pre-reported solution of Graetz problem. Their study explicitly described the role of Nusselt number and the entrance length with the Knudsen number and also developed the expressions to correlate the Nusselt number with the temperature field.

**Liu and Garimella [20]** in 2004 investigated liquid flow through microchannels experimentally as well as numerically for a particular range of hydraulic diameter and Reynold's no. Friction factors for different values of hydraulic diameter were assessed. Pressure drop and pressure gradient for different values of R e were plotted to understand the flow characteristics. Results of this work indicate that the conventional concept of slip and no-slip flow which can be used to predict flows through microchannel for the given range.

**Tretheway and Meinhart [21]** in 2001 measured the velocity profiles of fluid through hydrophobic microchannel walls using Micro-resolution velocimetry for particle image capturing. For hydrophilic surface, the velocity profile was well consistent to Stroke's equation and no-slip boundary condition. But for hydrophobic microchannel surface, an apparent slip velocity was found on the solid surface. In this study, the slip velocity was measured as a percentage of free-stream velocity yielding a slip-length (in  $\mu\text{m}$  scale). They concluded that for the higher length scale slip flow can be neglected, but it is obvious to be taken into consideration for micro and nano-scales.

**You, Theng and Jing [22]** in 2007 studied the role of boundary slip conditions and viscosity on the stability of mean velocity in micro channel. The microchannel walls of both similar and different material were taken into consideration. Navies slip conditions used to determine boundary slip conditions used to determine boundary slip condition. It was obtained from

numerical result that boundary slip is always helpful in stabilizing the flow. On the other hand, apparent viscosity always destabilizes the flow. It was also concluded that the boundary slip is strongly resisted by the interaction between close-wall molecules of wall and liquid.

**Kashaninejad, Chan and Ngugen [23]** in 2013 prepared a slip-flow model in parallel-plate micro channels analytically. The whole study was done in two parts. In the first one classical relationship depicting different flow parameters had been extended to general cases containing different slip lengths at both sides of parallel plate channel wall. In the second one, the slip length of the flow was analytically qualified. The findings of the paper show the guidelines for the analysis of slip flow in parallel plates micro channels both theoretically & experimentally.

**Tang and ye Taw [24]** in 2010 numerically investigated the electro viscous effect on non-Newtonian fluid in microchannels with the help of electric potential field and the Lattice Boltzmann methodology. The electro viscous effect was found to be dependent significantly on rheological character of fluid and the power-law exponent. The velocity profile and the electro viscous force behaviour were studied for shear thinning fluid. Moreover, electro viscous effect was found to be dependent on, the Debye length to channel height ratio, and the effect becomes weaker when the ratio is very small.

**Avsee, Vertie and Naterer [25]** in 2011 presented an expression for fluid flow and production of entropy in micro channels of different shape. Velocity profiles of flow in rectangular in graphical form. The significance and corresponding temperature variation were well depicted in paper.

**Shakir et.al. [26]** in 2011 have done a numerical investigation for microchannel with slip condition. Navier-Stokes equation was solved with the help of the slip boundary condition for a counter flow heat exchanger in micro dimensions. Operating parameters like pressure drop, slip velocity and temperature were analysed to find out the effectiveness of the device when the dimensionless parameters like Reynold's no, Knudsen no, Nusselt no etc. were varied to find out the slip flow characteristics.

**Yazdi et. al. [27]** in 2014 analysed power law model for non-Newtonian fluid flow through micro-patterned surface. A combination of no-slip and slip boundary condition is applied for open and open parallel microchannels respectively. Slip coefficient and power law index plays an important role in entropy generation locally along the surface. A relation between slip coefficient and entropy was established to find the critical value to find out the minimum production of entropy.

**Busheri et. al. [28]** in 2015 have extended the concept of slip flow in the application of heat sink made of microchannels. Boundary conditions for temperature jump along with the slip boundary condition were implemented. It was noted that heat sinks in slip flow regime have a noteworthy value of temperature jump.

**Kountouriotis et al. [29]** in 2016 found the effect of slip phenomena on the flow of Newtonian Poiseuille fluids. Navier slip boundary conditions have been employed. It was observed that in entrance region the effect of slip is stronger. Two expressions of development length were proposed for centerline and wall separately. It was noted that due to the presence of slip, flow development has a slower value at the vicinity of the wall. For this work, a generalized concept can be drawn for the Newtonian fluid flows.

**Ferras et. al. [30]** in 2014 worked on viscoelastic fluid of Newtonian nature in conjunction of slip boundary condition near microchannel walls. Slip condition proposed by Navier have been utilized along with the slip coefficients in dimensionless form. This work reported values for low Reynolds no. At the higher values, due to high shear stress gradients near wall the simulation could not converged. It was noted that due to the presence of slip, the possibility of the corner vortex is low.

**Ashrafi et. al. [31]** in 2020 employed Homotopy perturbation method to find an analytical solution. This solution can be applicable for Newtonian fluids for a porous flat plate. Governing equations of momentum and energy were solved by the proposed method and an analytical solution was achieved to find out the distribution of velocity and stress in the flow field.

**Nishad et. al. [32]** in 2016 applied boundary element method for the slip induced microchannels. Steady flow in two dimensional fluid flow fields in slip regime was simulated by the application of the slip boundary condition of Navier. On the basis of slip length slip flow have been divided into two subgroups. The prominent effect of slip length on the microchannel flows was noted and the effectiveness of boundary element method has been appreciated to find out the solutions of this kind.

**Shojaeian and Dibaji [33]** in 2010 performed a numerical analysis on the slip flow in triangular microchannels. They considered three dimensional flow field and found flow characteristics in slip regime. Navier-Stokes equation was used by the application of slip boundary condition and temperature jump. Dimensionless numbers like Knudsen No., Reynolds No., Poiseuille No. and Nusselt No. are examined for fixed aspect ratio of the triangular microchannel. It was noted that

for low Re the effect of Nu can be observed. When Kn is increased, consequently Nu also in the increasing mode. Poiseuille no. is also examined for fixed aspect ratio and different values of Re in the range of 1-15.

**Nagayama et. al. [34]** in 2017 assessed the effect of microchannel length scale and its decreasing value on liquid flow having single phase through microchannels to observe the Continuum breakdown at solid-liquid interface. Corrective heat transfer was considered along with the flow of liquid fluid of single phase to find out the expression of slip length at the vicinity of the solid liquid interface. An experimental set up with microchannel section was utilized and the variation of non-dimensional parameters like Poiseuille No., Nusselt No. was observed for a range of hydraulic diameter.

**Öztürk and Kahveci [35]** in 2016 studied heat transfer of laminar flow in steady fully developed situations. They introduced nano particles in the fluid of water based Copper and alumina nanoparticles mixed fluid. Governing equations were solved using slip boundary condition. The flow simulation was done through a parallel plate kept  $2H$  distance away. Velocity profiles drawn from this work indicate the extent of slip through the channel. It was noted, that the introduction of nanoparticles has a prominent effect for velocity field.

**Zhang et. al. [36]** in 2016 assessed the fluid flow characteristics of single phase liquid flow through microchannels experimentally at the very low values of Reynolds no. Deionized water mixed with kerosene was passed through rectangular microchannels for a hydraulic diameter of range between  $5\ \mu\text{m}$  to  $17.4\ \mu\text{m}$ . It was noted that the centerline velocity of the fluid may reach up to  $1\text{mm/s}$  when the Re is varied in the range of  $10^{-5}$  to  $10^{-2}$ . The linear variation of pressure drop was observed with the relation of average velocity. Friction factors were also assessed and micro PIV was used to observe velocity field and the flow field inside the microchannels.

**Yang et al. [37]** in 2019 found the flow characteristics for rheological fluids when they pass through microchannels. The pressure drop values of non-Newtonian fluid flow were measured experimentally with the help of sensors. Flow characteristics like flow rate, viscosity and other fluid parameters were noted in connection with pressure drop across microchannels. Power law was used to find out the apparent viscosity and shear rate near wall. Velocity profiles for the different values of power law index and consistency index were observed and used for conclusion.

**Barkhorderi and Etemad [38]** in 2007 have done numerical analysis to observe flow of non-Newtonian fluids through microchannels of circular cross section. Power law model is analyzed along with slip boundary condition to model steady, axisymmetric, laminar and incompressible flow through microchannels. Governing equations in dimensionless form are used to find out the effect of slip coefficient Reynolds no. and friction factors. Also a study has been made to find out the role of power law index on slip phenomena.

**Chakraborty [39]** in 2008 analyzed the flow of blood as a non-Newtonian fluid in a channel of microfluidic device. Hydraulic opposition near wall was investigated in a variable mode. This work demonstrated the possibility of the transport of non-Newtonian biological fluids like blood through microchannels. In this work a generic mathematical model is proposed which can be applied to analyze macromolecular (DNA or RNA) transport mechanism and for the micro flows of non-Newtonian fluids.

**Anna [40]** in 2008 analyzed non-Newtonian fluid like polymer in microscopic level to find out the shear rate for polymer chains with a special reference to Deborah number ( $De$ ). It was noted that dimensionless shear rate have a notable influence on the non-Newtonian fluid flow in microdevices. It was also found that two dimensionless no.  $De$  and  $Re$  influence the flow in microchannels.

**Etemad [41]** in 1995 conducted a comparative study between computational and experimental results of steady, laminar flow of non-Newtonian fluids through straight channels of circular and non-circular cross sections. No slip boundary condition was applied at the channel wall for steady, laminar flow to find out velocity profiles, pressure drop etc. Power law was used to model the non-Newtonian fluid. The effect of power law indices were also observed for flow characteristics and heat transfer performance.

**Muzychka and Edge [42]** in 2008 investigated the laminar flow of a non-Newtonian fluid in a microchannel and non-circular ducts. A simple model had been proposed for power law fluids. It had been shown that dimensionless wall shear stress can be expressed as a function of duct shape by means of square root of cross section area and a newly introduced characteristics length scale. The developed model is capable to predict pressure drop in a duct having non circular cross section.

**Niu, Fu and Tan [43]** in 2012 theoretically investigated the heat transfer and slip flow of a nanofluid of non-Newtonian behaviour in a micro tube. For describing non-Newtonian

characteristic, power law rheology had been adopted. The volumetric flow, velocity profile and Nusselt number had been calculated for different slip length and volume fraction of nanoparticles. It is found from the obtained results that the effect of volume fraction of nanoparticle on fluid flow highly connected to gradient of pressure, whose characteristics are different from the Newtonian nanofluid flow. The temperature profile in axial direction of the nanofluid flow at a constant wall temperature had been obtained by the aid of power series solution. The Nusselt number (local) had also been determined to represent heat transfer rate of nanofluid.

**Mansour, Kawahara and Sadatomi [44]** in 2015 experimentally investigated two phase flows of a gas-non-Newtonian liquid rectangular microchannel placed horizontally. The hydraulic diameter of the channel was 0.235 mm, width 0.24 mm and depth of 0.23 mm. A gas-liquid mixer had been used to mix liquid and gas in the microchannel. Nitrogen gas and Polyacrylamide aqueous solutions had been used as test gas and non-Newtonian liquids. The bubble length, bubble velocity, liquid slug length due to friction and flow characteristics had been studied thoroughly. The experimental data had been compared to those of the two-phase flow of gas and liquid. In case of Polyacrylamide aqueous solutions, rheological properties had been found to affect the measured flow parameters significantly. The Lockhart-Martinelli method had been used to correlate frictional pressure drop (2-phase) with a newly developed friction multiplier (2-phase) as a function of rheological index and void fraction.

**Sajadifar, Karimipour and Toghraie [45]** in 2016 numerically studied heat transfer and fluid flow of a non-Newtonian nanofluid through a micro tube taking temperature jump boundary conditions and slip velocity into consideration. Carboxymethyl cellulose-Aluminum oxide aqueous solution had been used as test solution. Length (5 mm) of the tube was chosen long enough compared to the diameter (0.2 mm). The effects of slip co-efficient, nanoparticle volume fraction, Reynolds number had been investigated on temperature jump and slip velocity. Suitable validation had been presented in favor of achieved results. The obtained results had been represented as dimensionless velocity and temperature profiles, local and averaged Nusselt number.

**Sarabandi and Moghadam [46]** in 2017 investigated power-law fluids to find out non-Newtonian flow characteristics in a circular microchannel considering slip boundary conditions and heat flux of constant value in the wall. Effects of thermal and hydrodynamic key parameters

as well as slip velocity on heat transfer had been thoroughly investigated. It had been found that both the Brinkmann number and flow behaviour index lead to the rising entropy generation but decreasing Nusselt number. As the slip co-efficient increases temperature difference between fluid and wall decreases, similar trend had been observed in cooling process also, for a range of Brinkmann number and slip co-efficient. Both the Bejan number and Nusselt number had been increased with the increasing slip co-efficient but entropy generation had decreased as well. The entropy generation had been found to increase with the increasing flow behaviour index or decreasing slip co-efficient.

**Vajravelu, Cannon and Rollins [47]** in 2000 investigated for the solutions of non-linear differential equations of second order in fluid flow with viscoelasticity in a rotating cylinder. This study was continued for the numerical and analytical solutions using the differential equations of power law fluid flow. By the use of Perturbation technique and the Schauder theory, uniqueness, existence and analytical results had been established. The differential equations of non-linear characteristics at boundary conditions had been solved numerically for different values of parameter  $\varepsilon$ , and some of the results had been represented graphically. It was found that the fluid velocities are affected by parameter  $\varepsilon$  significantly. The obtained analytical solutions had also been compared with the numerical solutions.

**Sharma, Gaikwad and Mondal [48]** in 2016 investigated the characteristics of entropy generation in microchannel flow of power law fluids under the effect of interfacial slip for Conjugate heat transport. Power law model had been considered for representation constitutive nature of non-Newtonian fluid. Accounting the influence of conjugate heat transport analytical solution had been made for the transport equations with (thermal) boundary conditions at the surface of exterior wall. For geometrical parameters like channel wall thickness, and thermo physical parameters like Peclet number, Biot number, and optimum value had been determined for minimum rate of entropy generation. The findings of the investigation could be helpful in the design of the devices used for micro-heat pipes, electronic cooling, micro-heat exchanger etc.

**Trebotich, Chang and Liepmann [49]** in 2001 had presented a model depending on the mechanism of blood flow at the MEMS length scale (10 to 100  $\mu\text{m}$ ), which represents the size of an arteriole. Investigation had been done on the use of simplified model of power law for blood flow in microchannel with cross-section  $200 \times 60 \mu\text{m}$ , at the rate of 2.5 to 100 ml/min. The microchannel used was straight, had a bend at  $90^\circ$  angle and 2 to 1 sudden contraction in



transverse direction. Numerical simulations had been done for pressure vs. flow rate of blood in microchannel which had been compared with experimental results. The study had suggested that the modelling of blood flow in this particular configuration and dimensions of 100  $\mu$  can be performed with simplified constitutive model in some cases with some further refinements.

**Zhang, Xie, Zhang and Xie [50]** in 2016 had studied the fluid flow and heat transfer characteristics of a non-Newtonian nanofluid in a heat sink consists of rectangular microchannel with protrusions of teardrop shape.  $\text{Al}_2\text{O}_3$ -water nanofluids had been used, which were defined by power law model. By analyzing temperature distributions and limiting streamline structures, heat transfer and flow characteristic had been analyzed. By Nusselt number and Fanning friction factor parameters, the thermal performance had been evaluated. The study showed that the combination of  $\text{Al}_2\text{O}_3$  aqueous solution and teardrop protrusion structure can strengthen the heat transfer with minimum pressure loss. Nanofluid with volume fraction of 3.5% had been used for the microchannel to obtain best overall thermal performance.

### **2.3 Applications of magnetohydrodynamics (MHD) in slip flow**

In last few decades the applications of MHD in the field of fluid mechanics has a notable increase of use. From macro to micro, in every flow regimes, researchers and scientists have worked to explore the nature and characteristics of fluid flow which is under the influence of MHD. Following are the examples of such works which have extensive research to find out the effect of MHD in modern engineering fluids and biofluids.

**Davidson [51]** in 1999 showed have MHD can be applied in processing of various engineering materials which includes not only ferrous materials but also non-ferrous materials. This work explains how MHD can be applied for stirring, melting and pumping. Metals like steel, aluminum and other alloys can be handled by MHD in process metallurgy. With the help of MHD how Ekman pumping works is also described in this work.

**Lemoff et. al. [52]** in 1999 demonstrated the operation of an AC micro pump operated by Magnetohydrodynamic (MHD) power. The Lorentz force had been used for propelling an electrolytic solution along a Silicon-etched microchannel. The operational theory and fabrication of micro pump were thoroughly demonstrated. The pump having no moving parts, but able to produce continuous flow, was compatible with biological specimens.

**Chaabane, Bouras and Nasrallah [53]** in 2007 investigated the performance of magnetohydrodynamic pump and reported a numerical method. The pump was associated with Faraday electrode configuration and a 2-D finite difference scheme had been used for evaluation. The pressure–velocity relation of electrolytic solution was formulated by numerical simulations. The reported method achieved quite well expected result for pressure distribution and velocity along the MHD duct. The results obtained from the investigation showed that the pressure distribution and velocity field of the flow are directly affected by externally applied magnetic field.

**Molokov and Reed [54]** in 2003 investigated the MHD flow of liquid metals under different (non-uniform) magnetic fields in circular ducts. The investigation was associated with the reference to liquid metal blankets of fusion reactors. The study continued with keeping the Hartmann numbers in the range between 50 and 2000. The validation of high-Ha model was also discussed in predicting the flow behaviour for intermediate Ha values. The inertia effect coming from the magnet at the entrance and exit of duct had also been investigated.

**Öztürk [55]** in 2014 investigated analytically the Slip flow (MHD) transfer of heat of a viscous fluid conducted electrically between parallel plates under a constant heat flux and transverse magnetic field. The results for varying Knudsen number, Brinkman number and Hartmann numbers were thoroughly discussed. The role of magnetic field on fluid flow was studied. The inter-relation slip among Knudsen number, Nusselt number, Brinkmann number and Hartmann number were investigated in detail.

**Aoki, Maunsell and Schilz [56]** in 2012 investigated a rectangular macro pump filled with electrolyte fluid. Magnetic and electric field were applied on the fluid. The magnetohydrodynamic study was done upon the fluid conductor in the closed circuit. A 3D numerical MHD model had been generated with the help of Navier Stokes and Maxwell equations for the sample fluid. Both the experimental and numerical analysis was carried out to explain MHD behaviour. The findings of the study might be useful in bioengineering, maritime propulsion, mining field as well as in nuclear engineering field. This investigation proves the promising future of MHD properties.

**Kiyasatfar, Pourmahmoud, Golzan and Mirzaee [58]** in 2014 presented a MHD model for fluid motion in rectangular channel based on theory of steady state laminar flow to explain the behaviour of MHD flow in MHD pumps. The velocity and temperature distribution were

thoroughly investigated through the numerical solutions of the non-linear equation of motion and energy. A code based on finite difference approximation was generated and used for analysis. Entropy generation rate had also been discussed. The simulated results of the work were compared with the experimental data.

**Khodak [59]** in 2017 had done a numerical analysis for the flow rate of 2D and 3D laminar flow in square duct by modifying CFD codes. This work applied magnetic field using ANSYS code which is a reliable tool for analysis. Liquid metal was considered as working fluid. Results of this work show a good agreement with the analytical solutions for a fully developed 2-D laminar flow as well as for a 3-D flow.

**Hasan, Ali and Tfah [60]** in 2016 investigated the MHD flow of sea water and phosphate mixed saline solution numerically under different electromagnetic boundary conditions. Electric current and magnetic field of specified range was applied to investigate the role of MHD on heat transfer. From the results it had been found that velocity and flow rate are quite well affected by the magnetic and electric field. The sea water showed a higher flow rate and velocity as compared to phosphate based saline solution. Joule heating also had a small effect on temperature rise.

**Hasan et. al. [61]** in 2017 performed a numerical simulation to find out the channel geometry effect on MHD micro pump. Different cross sections like circular square etc. were used in the simulation to understand the geometry effect on velocity and flow rate. It was observed that circular cross section shows higher values of velocity and flow rate due to the absences of losses at corner geometry.

**Rana, Shit and Reza [62]** in 2021 numerically investigated the slip flow and heat transfer features as well as the MHD magnetic field on a wavy microchannel. The fluid was allowed to pass through a porous medium. Differential equations of non-linear nature had been formed to present velocity and energy distribution. The effects of porosity, electromagnetic force, and inertia parameter, wavy-walls amplitude on slip flow and thermal transport had been thoroughly investigated in the study.

**Krasnov, Boeck, Braider, Molokov and Bühler [63]** in 2016 did a numerical simulation pressure-controlled MHD flow in ducts by the help of finite difference method. The flow transition was studied in the ducts when magnetic field was applied. The magnetohydrodynamic effect was studied using dimensionless numbers like Hartmann no. and Reynolds no..

**Gao and Jian [64]** in 2015 analytically investigated MHD flow for Jeffrey fluid in circular microchannel. The solutions for both DC and AC operated magnetohydrodynamic pumps had been found analytically by the use of variable separation method. By the use of Lorentz force, one dimensional, laminar flow had been investigated for volumetric flow rate and velocity varying with Hartmann number, dimensionless time of relaxation and time of retardation in graphical representation. The investigation results were also validated by comparing with previous results.

**Oyekunle, Akolade, Agunbiade and Momoh [65]** in 2022 investigated the role of slip on MHD flow of a fluid reacting chemically through an inclined channel which is micro-annular. The Akbari-Ganji's method had been employed to model the dimensionless governing equations of flow and to solve semi analytically.

**Oztop, Al-salem and Pop [66]** in 2011 analysed convection in cavity heated with corner heater and under the influence of magnetohydrodynamic field. The flow was considered as laminar flow. The technique of Finite Volume had been used for solving the governing equations. The analysis was performed for varying Hartmann and Grashof numbers at Reynolds number  $Re=100$ . The temperature profiles, velocity profile, variation of local Nusselt number at different directions were represented graphically.

**Sharma, Singh and Kumar [67]** in 2014 investigated the heat transfer and MHD flow in cylinder of circular shape filled partially with porous media which does not follow the Darcy's law. The effect of Joule heating was introduced by magnetic field. Quasi-numerical method of differential transform had been used to solve differential equations combined for velocity and temperature of the fluid. MATLAB had also been used for derivation and computation of temperature and velocity profiles of fluid in saturated porous as well as clear fluid annulus region and the results were represented graphically. The Nusselt number and coefficient of skin-friction at the cylinder wall and at surface of inner cylinder had been computed and discussed thoroughly.

**Laxmi Narayana and Gangadhar [68]** in 2015 investigated 2 dimensional unsteady slip flow of second order for in viscous, incompressible micro polar fluid conducted electrically over an impermeable and vertical stretching surface under the influence of MHD. The effect of buoyance on the flow had also been studied. MATLAB had been used for the solution of highly nonlinear

ordinary differential equations. Numerical calculations had been carried out for different dimensionless parameters for the problem and were represented graphically.

**Rabbi, Saha, Mojumder, Rahman, Saidur and Ibrahim [69]** in 2010 investigated purely mixed convection in a cavity for 2 heater configurations numerically under external magnetic field. Ferro fluid ( $\text{Fe}_3\text{O}_4$ -water) had been used as a working fluid. The weighted residuals method of Galerkin was used to solve the equations. The heat transfer had been analyzed for wide range of dimensionless numbers and solid-volume-fraction of the fluid thoroughly.

**Shit, Ranjit and Sinha [70]** in 2016 developed a numerical model for peristaltic wave of MHD flow for biofluids through microchannel. The numerical model had represented the non-Newtonian flow properties of biofluids. The important features of electro-MHD flow through microchannels of a biofluid had been highlighted through the variations of different parameters (non-dimensional) like velocity, pressure gradient, pressure rise (per wavelength), Shear stress, and frictional force at walls, and stream function distribution. It was clear from the analysis that the biofluid flow and formation of trapping is highly influenced by electro-osmotic parameter and strength of external magnetic field. The variation of frictional force with velocity-slip at channel had also been discussed.

**Sharma, Singh and Kumar [71]** in 2018 studied a steady state axisymmetric incompressible MHD flow through a non-Darcy porous media filled in circular annulus. The effect of Joule heating had also been produced to analyze magnetic and fluid flow field (on heating convection). The non-linear differential equations coupled for heat transfer and fluid flow had been solved using Quasi-numerical method-the Differential Transform method. MATLAB had been used at different physical parameters for investigation of temperature and velocity profiles for porous zone and central fluid zone and the results had been represented graphically. The Nusselt number and coefficient of skin-friction at the annulus surface had been computed and represented graphically.

**Nagaraju, Garvandha and Ramana Murthy [72]** in 2019 investigated a hypothesis on 2D thermal behaviour of viscous, axisymmetric, Newtonian heat flow through a horizontal pipe under an external uniform suction in polar direction across pipe wall. Magnetic field was applied in the perpendicular direction to the channel wall and also a heat source on cylinder surface of uniform value. The homotopy analysis method had been used for the solution of velocity field expressed as stream function. The effects of different geometric and flow parameters had been

analyzed through graphical representation. The distribution of temperature with the variation of Prandtl number and Eckart number had been observed thoroughly. Pressure contours, Streamlines and isotherm had also been presented in the paper.

**Tulu and Ibrahim [73]** in 2020 studied the carbon-nano liquid slip flow for a stretchable disk with rotation under the effect of heat flux. Ethylene glycol had been used as a base fluid for both single wall and multiwall carbon nano tubes. The effects of magnetic field, velocity, nanoparticle volume fraction, stretching factor and thermal slip factor had been investigated thoroughly. Ordinary differential equations of nonlinear parameters were used for numerical solutions. The temperature and velocity fields, local heat transfer rate, skin friction coefficient had been investigated in graphical and tabular form and represented through embedded parameters.

**Sheikholeslami and Ali Farshad [74]** in 2021 investigated absorber tube containing six lobes with combined tabulators. Hybrid nanoparticles had been added to the sample fluid to increase the productivity of solar collector system. Twisted tape and helical coil had been coupled together. For 3D simulation FVM had been used and homogeneous model had been used for nanofluid. For turbulent flow K- $\epsilon$  model had been employed. The effects of nanoparticle dispersion had been investigated. Nanofluid forced convection in the presence and absence of the tabulator had been verified. The benefits of six-lobe tube over circular tube were demonstrated by contours and plots.

**Buren, Jian, Chang, Liu and Zhao [75]** in 2016 investigated a time periodic AC MHD slip flow in microchannel having sinusoidal wall roughness, applying perturbation method for velocity and electrical potential. The influence of slip length, wall roughness, Hartmann number and frequency of electric potential on slip flow had been investigated both theoretically as well as graphically. The velocity distributions had been found to be disturbed by wall corrugation, depending on the shape of channel [phase difference  $\theta$ ]. The existence of phase lag  $x$  had been found between applied electric potential and velocity, resulting from momentum diffusion, which significantly varies with slip length ( $\beta$ ), non-dimensional frequency ( $\Omega$ ), wave number ( $K$ ), Hartmann number ( $Ha$ ) and phase difference ( $\theta$ ). The variation of amplitude of mean velocity with slip length, strength of electric field (parameters), wavenumber, frequency, phase difference of walls had also been investigated. The difference between flow characteristics for low frequency and high frequency had been studied also.

**Kiyasatfar and Pourmahmoud [76]** in 2015 investigated the steady laminar flow through square microchannels under transverse magnetic field. Modified power-law model was applied to solve the governing equations of momentum, energy and continuity through ADI scheme [Alternative Direction Implicit]. The temperature profile, velocity profile, products of friction factor and Reynolds number, Nusselt number had been computed for different values of shear rate parameters and flow index. The role of dimensionless numbers on temperature and velocity distributions had also been discussed.

**Gnaneshwara Reddy [77]** in 2017 investigated the effects of thermal slip and velocity on magnetohydrodynamic blood flow of third order through irregular channel filled with porous media with heterogeneous or homogeneous reactions. The flow had been observed under large wavelength and low value of Reynolds number. Mathematica software package had been used for numerical solution of dimensionless governing equation of flow with the boundary conditions. The effect of sundry parameters on fluid temperature, axial velocity, concentration characteristics had been represented graphically and also in tabular form. This study has significant application in biomedical engineering for thermal therapy.

**Sushma, Samuel and Neerja [78]** in 2018 studied the impact of unsteady mass and heat transfer on magnetohydrodynamic blood flow numerically, considering the slip effect. The shooting method had been used for the solution of non-linear differential equations coupled for concentration and thermal flow of unsteady blood flow. The heat transfer, mass transfer and impact of different controlling parameters on the flow of blood had been presented graphically and validated with adequate data.

#### **2.4 Applications of MHD induced slip flow for modern fluids for engineering applications**

Presently, MHD is being applied to control modern engineering fluids and bio fluids. Nanoparticles which are conducting in nature are being mixed with base fluids to have a flow through microchannels which are under the influence of externally applied magnetic fields. There are also biofluids which are conducting in nature. They are being controlled through fluid devices by the help of MHD. Follow are the examples of such works which are referred to do an extensive study on the modern applications of MHD.

**Andreev, Kolesnikov and Thess [79]** in 2006 experimentally investigated the flow of liquid metal through a rectangular channel under the application of non-homogeneous magnetic field.

Depending on electric potential and local velocity three different flow regions had been identified. The variation of flow characteristics and velocity profile with applied magnetic field in these three different regions had been observed thoroughly. Eutectic alloy had been used as working fluid and permanent magnets having finite dimensions had been used for non-homogeneous magnetic field. The experimental data presented in this study may be useful for numerical simulations of turbulent magnetohydrodynamic flows.

**Ghasemi, Aminossadati and Raisi [80]** in 2011 investigated natural convection in a square enclosure, consists of  $\text{Al}_2\text{O}_3$ -water nanofluid. Two numbers of horizontal adiabatic walls and two numbers of isothermal walls placed vertically at two different temperatures with completely bounded enclosure. The variation of flow nature and temperature distribution with the pertinent dimensionless numbers had been investigated.

**Hoseinzadeh, Heyns and Kariman [81]** in 2019 numerically investigated laminar flow, turbulent flow and pulsating flow in a 2-D channel. For the purpose they choose  $\text{Al}_2\text{O}_3$  water nanofluid. Various temperature distribution and fluid flow analysis were done. The work also finds the role of volume fraction of nano fluids. It was noted that the mixing of nanofluid particles in liquid flow has a significant effect for laminar as well as turbulent flow.

**Lalami, Afrouzi and Moshfegh [82]** in 2018 investigated the flow of nanofluids in microchannel under transverse magnetohydrodynamic field. A standard model was used for the investigation of flow in the microchannel with super hydrophobic or hydrophilic walls. Water nanofluid flow had been used as experimental fluid. Velocity Field had been resolved and temperature field had been resolved. Keeping the Reynolds number as constant at 100, different Hartmann numbers ( $\text{Ha} = 0$  to 30), slip coefficients ( $B = 0$  to 0.1) and volume fractions of nanoparticles ( $\Phi = 0$  to 20%) had been investigated considering temperature and velocity slippage.

**Escaudon, Bautista, Santiago and Mendez [83]** in 2014 studied the asymptotic solution of velocity profiles and shear stress distributions of non-Newtonian fluid flow in a flat parallel plate microchannel under a combination of electro-osmotic and magnetohydrodynamic micro pumps. The effect of Hartmann number and viscoelastic parameter on fluid flow had been investigated. A set of non-linear differential equation had been formed by combining boundary conditions, momentum equation and constitutive rheological model to solve shear stress. The values of Hartmann number in the asymptotic solution,  $\text{Ha} < 0.01$ , were found to attain a good



approximation. The study contributed to the better understanding of the coupled flow mechanism for design of any microfluidic system. The combined effect of electric and magnetic field on fluid flow in microchannels might be useful for chemical and medical applications, if electrical conductivity considered within allowable limits with no large changes in temperature of fluid.

**Sheikholeslami, Gorji-Bandpy and Ganji [84]** in 2013 numerically investigated the nanofluid flow of Al<sub>2</sub>O<sub>3</sub>-water under magnetohydrodynamic effects and the transfer of heat in a concentric semi annulus enclosure. Lattice Boltzmann Method had been applied for the solution of governing equations. Already available correlations had been used for the calculation of viscosity of the nanofluid. The numerical study had been carried out for different numbers of Rayleigh number, Hartmann number, volume fraction of nanoparticles etc.

**Das, Jana and Makinde [85]** in 2014 studied MHD slip flow of boundary layer on a vertically placed sheet and heat transfer of a nanofluid with non-uniform absorption on heat generation. The set of coupled ordinary differential equation of non-linear characteristics was solved numerically. Numerical investigation had been carried on for temperature, fluid velocity, shear stress and heat transfer. It had been found that temperature and velocity profiles were significantly affected by different pertinent parameters which had been thoroughly discussed in graphical and tabular form.

**Elelmy and Elgazery [86]** in 2020 investigated the blood flow of non-Newtonian nanofluids under magnetohydrodynamic field with slip effects and heat transfer. A mathematical model had been predicted numerically for blood flow in arterial valve with growth of bacteria. Non-Newtonian nanofluid of Casson micro polar flow in arterial valve for 2D with variable properties had been used for the investigation. The heart valve modified with prosthesis through the transfer of heat with induced magnetic field translational attraction combined with the influence of slip.

**Arjun and Rakesh [87]** in 2017 studied flow behaviour and thermal models using water and alumina nanofluid in single phase flow in a microchannel of circular shape. A CFD based on finite volume method had been used and modes had been solved by the use of fluent solver. The two dimensional axisymmetric geometry along with a structural mesh and nodes of 100×18 had been used for flow of single phase with alumina nanoparticles of 23 nm diameter. In laminar and turbulent zone, standard K-ε and viscous laminar models had been used for the prediction of steady temperature. Pressure drop and Nusselt number had been formulated. The analytical data reported in the study had been compared with the predictions.

**Arani, Sheikhzadeh and Arani [88]** in 2014 studied thermal and fluid flow characteristics of alumina nanofluid mixed with water in a square lid-driven enclosure numerically. The non-Newtonian behaviour of the nano-fluid had been demonstrated thoroughly. For the estimation of the viscosity of fluid, a new model had been proposed, using experimental data from Hong and Kim. The obtained results from the study had been compared with the Newtonian behaviour. Gr number was in the range of 104 to 106 and Solid volume fraction was  $5.0 \geq \Phi (\%) \geq 0.0$ . The diameter of nanoparticles was 50 nm and Prandtl number was 6.1 for the base fluid. Heat transfer was found to increase with increase in solid volume fraction at any Re. A considerable amount of decrease in Nusselt number was found at non-Newtonian behaviour than Newtonian behaviour.

**Sheikholeslmi, Hayat and Alsaedi [89]** in 2016 investigated the thermal characteristics of alumina nanofluid flow in an enclosure under the effect of applied magnetic field. For the simulation of thermal and fluid flow characteristics of nanofluid, previously available correlations had been used. Finite element method based on control volume had been used for solving the governing equations. The role of dimensionless numbers on the fluid flow was studied. The characteristics of heat transfer had also been examined. The increase in heat transfer takes place with the increment in viscous dissipation parameter, Hartmann number, radiation parameter.

**Raja Sekhar and Sharma [90]** in 2015 have studied the thermal characteristics of alumina nanofluids mixed with water for low value of particle concentrations. A nonlinear variation in viscosity is observed when the particle concentration is changed. This experimental work demonstrated the changing nature of viscosity, relative viscosity and effective viscosity when temperature, particle diameter and particle concentration is changed.

**Karimipour et. al. [91]** in 2016 compared silver nanoparticles with alumina nanoparticles and find out the advantages of using alumina nanoparticles for better heat transfer at same values of Re. The whole analysis is done for the values of Ha up to 40. They have used MHD in such a fashion that the induced Lorentz force acts in opposite direction and the results yields for higher values of Ha centerline velocity decreases.

**Kumar et. al. [92]** in 2017 used ferrous nanofluids in slip flow regime and observed the effect of MHD. They incorporated Brownian motion and thermophoretic forces in the governing equations. Ferrous nanoparticles have been noted as the factor in heat transfer improvement.

They also observed slip flow have a significant role in velocity and concentration field. From this study it is observed that nanofluids have ability which can change the velocity.

**Das et. al. [93]** in 2017 used pure alumina nanoparticles mixed with water and they have compared the results when copper nanoparticles mixed alumina nanoparticles mixed with water flows through porous channel under the effect of magnetic field. Transverse magnetic field is used to reveal the fluid velocity enhancements, heat transfer enhancement, etc. for hybrid nanoparticles of copper and alumina. It was noted that hybrid nanoparticles have better performance in heat transfer for cooling systems.

**Gangadhar et. al. [94]** in 2020 assessed the heat transfer enhancement of hybrid nanoparticles in the range of 20% to 50% more as compared to the conventional non-hybrid nanoparticles suspension under transverse MHD flow. The work also assessed the influence of particle concentration on velocities which increase skin coefficient factor and heat transfer at the vicinity of the wall.

**Ghalambaz et. al. [95]** in 2019 worked on copper mixed alumina nanoparticles in a cavity to find the natural convection under the effect of MHD. They analyzed the streamline patterns for a range of Hartmann no 200 and Rayleigh no (Ra). They found the importance of nanoparticles concentration on heat transfer performance under MHD.

**Iftikar et. al. [96]** in 2019 used alumina and copper nanoparticles mixed with water to find out the slip effects under MHD for physiological delivery. For the purpose, unstable peristaltic motion is considered through non uniform circular microchannel. For increased slip parameters, higher impact is noted for hybrid nanofluids. The results of this work can be useful for drug delivery using peristaltic pump of micro order.

**Jain and Bhargava [97]** in 2020 applied mesh free method for numerical simulation to find out the convection of non-Newtonian nanofluid through wavy enclosure. Flow behaviour index ranging from 0.2 to 1 and Hartmann no up to 50 is used. This work demonstrates that the applicability of mesh free method in this area for numerical simulations.

**Qomi et. al. [98]** in 2020 observed pulsating flow of hybrid nanofluids under MHD in a microchannel for Re 50-100 and ha 0 to 50. This numerical simulation used sinusoidal function for the excitation of inlet laminar flow. An increase of heat transfer by 350% is observed when Re changes its value from 100 to 500. It is noted that this work can be applied for micro cooling systems.

**Brinkman [99]** in 1952 had worked out on the viscosity of suspensions and solutions and a set of mathematical expressions was derived for continuous mediums. The relations of viscosity for a different concentration were found out and these relations were proven to be very useful to find out the expressions of viscosity of fluids having suspended particles.

**Bazinet et. al [100]** in 2004 performed a set of experiments for optimum design and quality control for rheological characteristics of whey protein with a special reference to pH and protein concentration. A relation between shear rate, viscosity and shear stress of protein solutions were worked out. Power law indices like flow behaviour index and consistency index, are found to be two major influential parameters which affect apparent viscosity. Various sets of physical data was examined and tabulated for a better understanding.

**Elbbesy and Hereba [101]** in 2016 investigated the values of flow behaviour index and consistency index for whole blood using power law. The process involves experimental procedure for a set of 20 blood samples to find out the viscosity under the range of shear rate values. Power law indices were calculated using shear rate and viscosity plot. From the experimental data it was concluded that blood flow behaviour is a kind of a non-Newtonian fluid flow. It was also noted that power law model is the best model which can describe the nature of blood flow.

**Shekarforoush et. al. [102]** in 2017 estimated power law indices experimentally for a shear thinning characteristics of Xanthan solution mixed with formic acid. The solution of xanthan in formic acid was in the range of 0.5 to 2.5 wt/vol %. The conductivity is also measured of these solutions along with flow behaviour index, consistency index viscosity, and shear rate. The results show us the development of new properties of a biofluids to make it a conducting fluid with the help of formic acid. These are the modern biofluids which are now being analyzed in labs to find their applications in modern engineering.

## **2.5 Scope and objective of the work**

According to the review of various literatures available, not many studies have been conducted on magnetohydrodynamic effect on wall slip for non-Newtonian fluid flow in microchannels. Although not many aspects in this context have been studied, the knowledge base is not extensive. But studies are still being done, which indicates the need for more in-depth investigation. Additional research is needed in number of areas.

The purpose is specified in the current work in a very specific and focused way, in a manner similar as stated. The objective of this work is to find out the role of MHD on slip velocity of non-Newtonian fluids. This work also includes a study of slip flow when flow behaviour index changed.

For these purpose fluid properties of xanthan solution in formic acid is used for the study. The objectives can be summarized as follows:

- i. A validation is planned to have a comparison of this work with the already available data in standard literature.
- ii. A mathematical analysis is planned before the numerical simulation of the present problem.
- iii. The present work is planned to investigate effect of wall slip in the flow of non-Newtonian fluids through microchannels.
- iv. It is also been planned to find out the role of magnetohydrodynamics on slip induced non-Newtonian fluids through microchannels.
- v. This work uses the fluid properties of xanthan solution in formic acid to have a reality check with the help of practical fluids.

To be in line with the objectives of the present work, problem analysis, mathematical analysis, numerical simulation, analysis of flow characteristics and dimensionless numbers etc. become important.

These features have been the subject of in-depth study to build a solid knowledge base that will assist practitioners in using magnetohydrodynamics in microchannels that handles non-Newtonian fluids in a more predictable manner, ensuring desired performance.

## MATHEMATICAL ANALYSIS AND NUMERICAL SIMULATION

---

### 3.1 Mathematical Analysis of Slip Induced Flow of non-Newtonian Fluids

Let us consider a fully developed, steady state, laminar flow of non-Newtonian fluid in a microchannel having circular cross section and having radius  $R$  as shown in Fig. 04. This flow is steady and incompressible in nature. Rotational symmetry has been considered which makes the flow two dimensional and axisymmetric in nature.

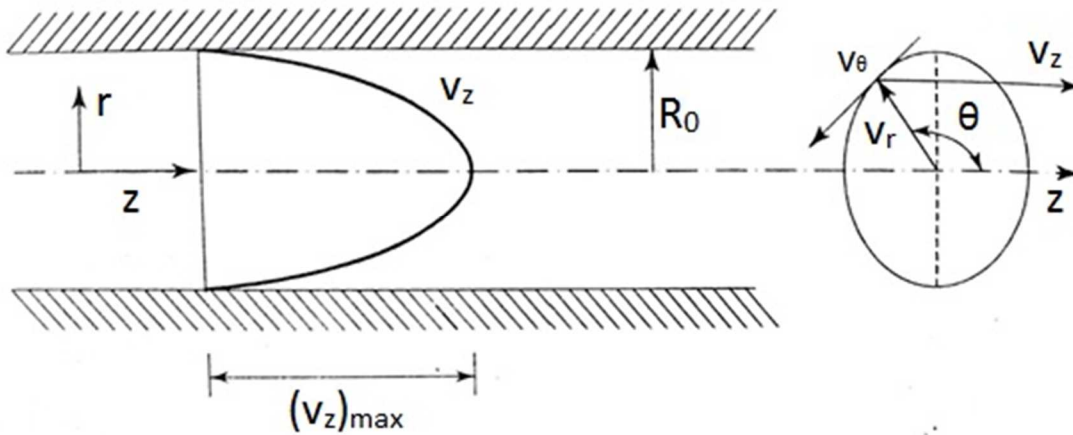


Fig. 04 Circular microchannel showing cylindrical co-ordinates

Let us consider  $z$  axis as the axis of the micro-tube along which non-Newtonian fluid particles travel. Therefore we can write,

$$v_z \neq 0, v_r = 0 \text{ \& } v_\theta = 0$$

Now, from continuity equation we get,

$$\frac{\partial}{\partial r}(v_r) + \frac{1}{r} \frac{\partial}{\partial \theta}(v_\theta) + \frac{\partial v_z}{\partial z} + \frac{v_r}{r} = 0$$

For rotational symmetry,

$$\frac{1}{r} \frac{\partial}{\partial \theta}(v_\theta) = 0 \text{ \& } \frac{\partial}{\partial r}(v_r) = 0$$

Therefore,  $\frac{\partial v_z}{\partial z} = 0$

or,  $v_z = v_z(r, t)$

or,  $v_z = v_z(r)$

Let us consider Navier-Stokes equation in cylindrical co-ordinates along r-z direction,

$$\rho \left( \frac{\partial v_z}{\partial t} + v_r \frac{\partial v_z}{\partial r} + \frac{v_\theta}{r} + u_z \frac{\partial v_z}{\partial z} \right) = - \frac{\partial P}{\partial z} + \rho g_z + \mu \left[ \frac{1}{r} \frac{\partial}{\partial r} \left( r \frac{\partial v_z}{\partial r} \right) + \frac{1}{r^2} \frac{\partial^2 v_z}{\partial \theta^2} + \frac{\partial^2 v_z}{\partial z^2} \right]$$

Invoking  $v_r=0, v_\theta=0, \frac{\partial v_z}{\partial z} = 0$  &  $\frac{\partial}{\partial \theta}(\text{any quantity}) = 0$  and neglecting various terms of Navier-Stokes equation for steady flow we get,

$$\begin{aligned} \mu \left[ \frac{1}{r} \frac{\partial}{\partial r} \left( r \frac{\partial v_z}{\partial r} \right) \right] - \frac{\partial P}{\partial z} &= 0 \\ \frac{1}{\mu} \frac{\partial P}{\partial z} &= \left[ \frac{1}{r} \frac{\partial}{\partial r} \left( r \frac{\partial v_z}{\partial r} \right) \right] \\ r \frac{\partial P}{\partial z} &= \left[ \frac{\partial}{\partial r} \left( r \mu \frac{\partial v_z}{\partial r} \right) \right] \\ r \frac{\partial P}{\partial z} &= \left[ \frac{\partial}{\partial r} (r \tau_{rz}) \right] \end{aligned} \quad (1)$$

From Newton's law of viscosity we get the following form of the expression of shear stress for cylindrical coordinates working in fluid

$$\tau_{rz} = \mu \frac{\partial v_z}{\partial r}$$

In cylindrical co-ordinates, this expression can be written for the shear stress along z direction

$$\tau_{rz} = \mu \left( \frac{\partial v_r}{\partial z} + \frac{\partial v_z}{\partial r} \right)$$

For a steady flow with no radial component of velocity,  $\frac{\partial v_r}{\partial z} = 0$

We have,

$$- \tau_{rz} = \mu \left( \frac{\partial v_z}{\partial r} \right) \quad (2)$$

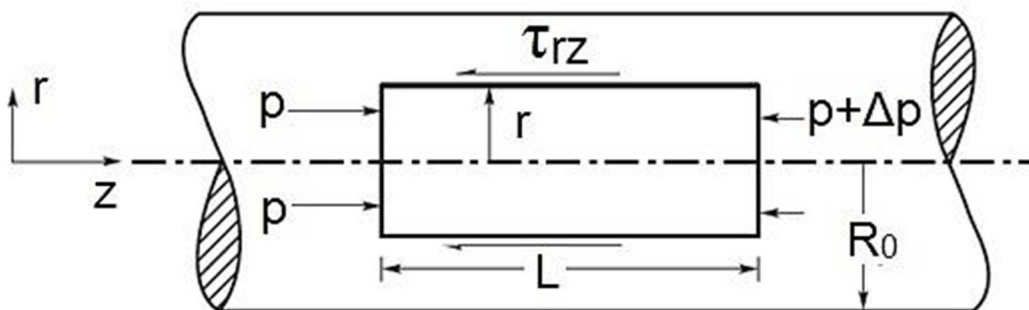


Fig. 05 Flow through a circular channel

With reference to the Fig. 05, the force balance on a fluid element located at a distance  $r$  can be expressed as follows considering no rotational velocity.

$$p(\pi r^2) - (p + \Delta p)\pi r^2 = \tau_{rz} \times 2\pi r L$$

$$\text{i.e. } \tau_{rz} = \left(\frac{-\Delta P}{L}\right) \frac{r}{2} \quad (3)$$

Again from Ostwald deWaele relationship of non-Newtonian fluid flow we know,

$$\tau_{rz} = K \left(-\frac{dv_z}{dr}\right)^n \quad (4)$$

$$\frac{\tau_{rz} \times dr^n}{m} = -(dv_z)^n$$

$$\left(\frac{\tau_{rz}}{m}\right)^{1/n} dr = -dv_z$$

$$dv_z = -\left(\frac{\tau_{rz}}{m}\right)^{1/n} dr$$

$$dv_z = -\left\{\left(\frac{-\Delta P}{L}\right) \frac{r}{2} \times \frac{1}{m}\right\}^{1/n} dr \quad \left\{\text{as we know from eqn (3), } \tau_{rz} = \left(\frac{-\Delta P}{L}\right) \frac{r}{2}\right\}$$

$$dv_z = -\left\{\left(\frac{-\Delta P}{L}\right) \frac{1}{2m}\right\}^{1/n} r^{1/n} dr$$

Integrating both sides of the above equation we get,

$$v_z = -\left\{\left(\frac{-\Delta P}{L}\right) \frac{1}{2m}\right\}^{1/n} \frac{r^{\frac{1}{n}+1}}{\frac{1}{n}+1} + \text{Constant}$$

$$v_z = -\left\{\left(\frac{-\Delta P}{L}\right) \frac{1}{2m}\right\}^{1/n} \frac{r^{\frac{1+n}{n}}}{\frac{1+n}{n}} + \text{Constant}$$

$$v_z = -\left(\frac{n}{n+1}\right) \left\{\left(\frac{-\Delta P}{L}\right) \frac{1}{2m}\right\}^{1/n} r^{\left(\frac{n+1}{n}\right)} + \text{Constant} \quad (5)$$

The Navier's slip boundary conditions can be summarized as follows:

$$\text{at, } r=R_0 \quad v_z=v_s$$

$$\text{at, } r=0 \quad dv_s/dr = 0$$

The non-dimensional form of the above boundary conditions can be stated as:

$$\text{at, } R=1 \quad v=\beta$$

$$\text{at, } R=0 \quad dV/dR = 0$$

Using the expressions (5) when boundary conditions are applied, we get the expression of velocity along z direction ( $v_z$ ).

$$v_z = v_s + \left(\frac{3n+1}{n+1}\right) \left\{1 - \left(\frac{r}{R_0}\right)^{\frac{n+1}{n}}\right\} (v_m - v_s) \quad (6)$$

Here mean velocity ( $v_m$ ) can be expressed as,

$$v_m = v_s + \left(\frac{n}{n+1}\right) \left(-\frac{\Delta P}{L} \frac{R_0}{2m}\right)^n R_0 \quad (7)$$



Following are the parameters in their non-dimensional form which are useful to find out the non-dimensional form of velocity  $V$ .

$$\frac{V_z}{V_m} = V, \frac{r}{R_0} = R, \frac{l}{R_0} = L, \frac{v_s}{v_m} = \beta, \frac{z}{R_0} = Z, \frac{p}{\rho v_m^2} = P, Re = \frac{\rho v_m^{2-n} r_0^n}{m}$$

Using the dimensionless quantities the above equation can be expressed as

$$V = \beta + \left( \frac{3n+1}{n+1} \right) \left\{ 1 - (R)^{\frac{n+1}{n}} \right\} (1 - \beta) \quad (8)$$

At centreline, where  $r/R_0 = R = 0$ ; the velocity reaches its maximum value of  $v_{max}$  which can be formulated as

$$V_{max} = \beta + \left( \frac{3n+1}{n+1} \right) (1 - \beta) \quad (9)$$

The expression of skin friction co-efficient can be written as

$$C_f = \frac{2 \tau_{rz} (r=r_0)}{\rho v_m^2} \quad (10)$$

Wall slip equation: For the momentum equation, Navier's slip condition is applied at the channel walls of the microchannels. The mathematical form of this boundary condition can be written as:

$$u_{s_{r=D_h/2}} = l_s \left( \frac{dv_z}{dr} \right)_{r=D_h/2} \quad (11)$$

### 3.1.1 Problem Statement

In this study, non-Newtonian fluid is modelled using power law. The flow is considered to pass through circular microchannel of diameter 400  $\mu\text{m}$ . The length ( $L$ ) of the circular straight microchannel is 20 mm. The analysis is done for entrance zone and developed section to understand the role of slip velocity on fluid flow. Slip velocity is presented in terms of slip co-efficient ( $\beta$ ) which is a ratio of velocity at wall to the average velocity. This work covers the effect of slip co-efficient for different values of flow behaviour index ( $n$ ). The problem under consideration is shown schematically in Fig. 06. The problem is considered to be an axis symmetric problem. Therefore the solution of the problem is done for the one half along the microchannel axis. Constant fluid properties are considered for the power law to model shear stress as described in equation (4). At microchannel entry, an uniform velocity  $(v_z)_e$  is considered.

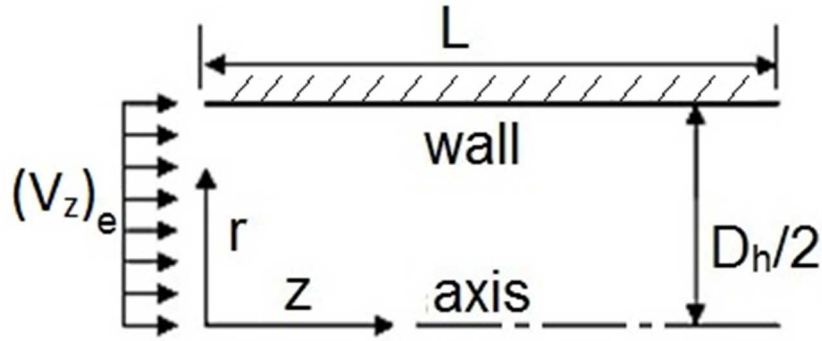


Fig. 06 Computational domain of the slip flow in circular microchannel.

### 3.2 Mathematical Analysis of Magnetohydrodynamics

With a reference to Fig. 06 from Navier Stokes equation for steady flow, the governing equation becomes,

$$\mu \left( \frac{\partial^2 v_z}{\partial r^2} + \frac{1}{r} \frac{\partial v_z}{\partial r} \right) = \frac{dp}{dz}$$

$$\frac{\partial^2 v_z}{\partial r^2} + \frac{1}{r} \frac{\partial v_z}{\partial r} = \frac{1}{\mu} \frac{dp}{dz} \quad (12)$$

Now let us consider the magnetic field of  $B_0$  strength has been applied on the fluid having  $\sigma$  electrical conductivity. This situation is shown in the figure below in Fig. 7

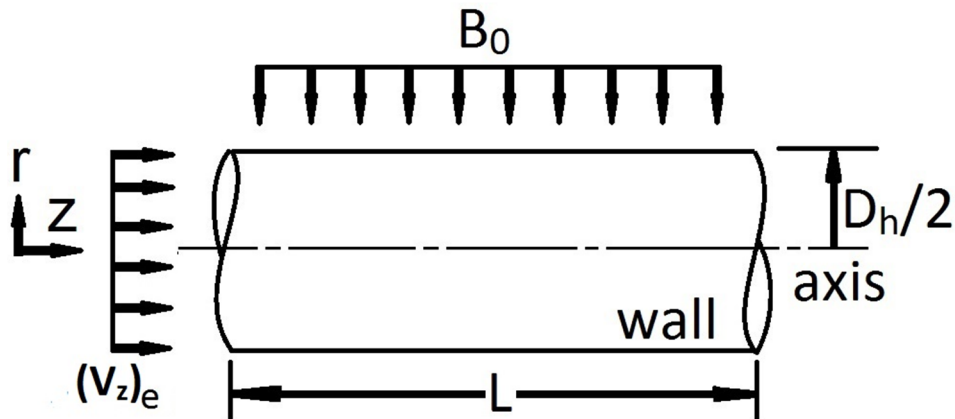


Fig.07 Schematic diagram of the flow field under the effect of externally applied Magnetic field

Under this geometrical configuration and assumptions, two dimensional and laminar equations for a steady flow considering a uniform magnetic field of strength  $B_0$  can be written as following.

Continuity equation:

$$\frac{\partial v_r}{\partial r} + \frac{\partial v_z}{\partial z} = 0 \quad (13)$$

Momentum equation:

$$\mu \left( \frac{\partial^2 v_z}{\partial r^2} + \frac{1}{r} \frac{\partial v_z}{\partial r} \right) = \frac{dp}{dz} + \sigma B_0^2 v_z \quad (14)$$

To make the equations dimensionless, let us introduce the following non-dimensional quantities

$$R = \frac{r}{D_h}; \quad Z = \frac{z}{D_h}; \quad V_Z = \frac{v_z}{v_{ze}}; \quad G = \frac{\frac{dp}{dz}}{\rho v_{ze}^2}; \quad H_a = B_0 D_h \sqrt{\frac{\sigma}{\mu}}$$

Writing equation (14) we get,

$$\begin{aligned} \frac{\partial^2 v_z}{\partial r^2} + \frac{1}{r} \frac{\partial v_z}{\partial r} &= \frac{1}{\mu} \frac{dp}{dz} + \frac{\sigma}{\mu} B_0^2 v_z \\ \frac{\partial^2 (V_Z v_{ze})}{\partial (R D_h)^2} + \frac{1}{R D_h} \frac{\partial (V_Z v_{ze})}{\partial (R D_h)} &= \frac{1}{\mu} G \frac{\rho v_{ze}^2}{D_h} + \frac{\sigma}{\mu} B_0^2 (V_Z v_{ze}) \\ \frac{v_{ze}}{D_h^2} \frac{\partial^2 V_Z}{\partial R^2} + \frac{v_{ze}}{D_h^2} \frac{1}{R} \frac{\partial V_Z}{\partial R} &= \frac{1}{\mu} \frac{\rho}{D_h} v_{ze}^2 G + v_{ze} \frac{\sigma}{\mu} B_0^2 V_Z \\ \frac{\partial^2 V_Z}{\partial R^2} + \frac{1}{R} \frac{\partial V_Z}{\partial R} &= \frac{\rho}{\mu} v_{ze} D_h G + \frac{\sigma}{\mu} B_0^2 D_h^2 V_Z \\ \frac{\partial^2 V_Z}{\partial R^2} + \frac{1}{R} \frac{\partial V_Z}{\partial R} &= Re \cdot G + H_a^2 V_Z \end{aligned} \quad (15)$$

Similarly, we can derive the dimensionless expression of the equation (13) which can be written as:

$$\begin{aligned} \frac{\partial v_r}{\partial r} + \frac{\partial v_z}{\partial z} &= 0 \\ V_R = \frac{v_r}{v_{ze}}, V_Z = \frac{v_z}{v_{ze}}, Z = \frac{z}{D_h}, R = \frac{r}{D_h} \\ \frac{v_{ze}}{D_h} \frac{\partial V_R}{\partial R} + \frac{v_{ze}}{D_h} \frac{\partial V_Z}{\partial Z} &= 0 \\ \frac{\partial V_R}{\partial R} + \frac{\partial V_Z}{\partial Z} &= 0 \end{aligned}$$

Similarly for equation (12) we can get the non-dimensional form:

$$\begin{aligned} \frac{\partial^2 v_z}{\partial r^2} + \frac{1}{r} \frac{\partial v_z}{\partial r} &= \frac{1}{\mu} \frac{dp}{dz} \\ \frac{\partial^2 V_Z}{\partial R^2} + \frac{1}{R} \frac{\partial V_Z}{\partial R} &= \frac{1}{\mu} \frac{D_h^2}{v_z} \frac{\rho}{D_h} v_{ze}^2 G \\ \frac{\partial^2 V_Z}{\partial R^2} + \frac{1}{R} \frac{\partial V_Z}{\partial R} &= \frac{D_h}{\mu} \rho v_{ze} G \end{aligned}$$

$$\frac{\partial^2 V_Z}{\partial R^2} + \frac{1}{R} \frac{\partial V_Z}{\partial R} = Re \cdot G \quad (16)$$

### 3.2.1 Physical Considerations Used for MHD Induced Slip Flow

A slip driven; non-Newtonian fluid flow has been considered through a circular microchannel. The diameter of the microchannel as compared to the length is very small. The fluid flowing through the microchannel is fully developed due to the sufficient length of the channel. The flow has been considered is axisymmetric, laminar, steady, and incompressible in which Ostwald-deWaele power law model is applied to analyze the flow characteristics of non-Newtonian fluid. All the fluid properties are kept constant at the time of analysis. Slip boundary condition is used at the microchannel wall. The axial coordinate,  $z$ , is considered along the length of the microchannel and along the radial direction 'r' coordinate has been considered as shown in Fig. 07. The length of the microchannel ( $L$ ) under consideration is 20 mm and the diameter of the microchannel ( $D_h$ ) is 440  $\mu\text{m}$ . The flow is affected by an external, constant magnetic field equal to a value varying from  $B_0 = 0.1\text{T}$  to  $0.4\text{T}$  in order to determine the effect of increasing value of field intensity. This magnetic field is applied perpendicular to the length of the microchannel. A unidirectional flow at the entry of the microchannel of intensity  $v_e$  is considered which is under the influence and application of an applied pressure gradient.

### 3.2.2 Fluid Properties

This work has been done by considering a fluid which exhibits simultaneous behaviour of non-Newtonian fluid and electrical conductivity. The present study reveals the fluid behaviour of Xanthan in formic acid solution (05 wt./vol%) when it is passed through a circular microchannel of sufficient length compared to the diameter. The properties of 0.5 wt./vol% xanthene polysaccharide are described in Table 1. The aqueous solution of Xanthan typically shows weak gel-like thixotropic properties. When this Xanthan is mixed with formic acid in different ratios the solutions show electrical conductivity. Xanthan gum is a type of extracellular heteropolysaccharide produced by a bacterium called *Xanthomonas campestris*. It contains glucose, mannose and glucuronic acid in the molar ratio of 2:2:1.

Table 01 Properties of Xanthan solution in formic acid (25 °C) [102]

Xanthan [wt/vol%]	$\rho$ (kg/m <sup>3</sup> )	n	K (kg s <sup>(n-2)</sup> /m)	Electrical conductivity ( $\sigma$ ) ( $\Omega\text{m}$ ) <sup>-1</sup>
0.5	1225	0.761	0.214	0.01343
1.0	1230	0.473	2.274	0.02657
1.5	1235	0.317	10.617	0.03567

### 3.3 Dimensionless Parameters

From the mathematical analysis it is understood that there are few dimensionless numbers which are necessary to describe the flow under consideration. Here is a brief description of these dimensionless numbers.

Reynold's Number (Re): This is the ratio between inertia force and viscous force of a fluid flowing through a channel. This dimensionless no is required in a mathematical analysis to describe the nature of flow through channel. Here nature of flow indicates whether the flow is laminar, transition or turbulent. When Reynold's no is less than 2000 then the flow is called laminar flow. In this analysis, the flow is laminar in nature that is, the Re is always less than 2000.

Fanning Friction Factor ( $C_f$ ): This dimensionless quantity is a ratio of local shear stress at wall, to the kinetic energy in the fluid at wall. This is also known as skin co-efficient factor. For a fully developed flow, in a closed channel it is given by,

$$C_f = \frac{\tau_w}{\frac{1}{2}\rho v^2}$$

Darcy Friction Factor (f): This is a dimensionless quantity used to describe friction losses in a channel. This is also known as Darcy-Weisbach friction factor. Darcy friction factor is four times than that of skin co-efficient factor.

Hartmann Number (Ha): This dimensionless quantity is a ratio of electromagnetic force to the viscous force of the fluid. This dimensionless number is required for the analysis of the fluids which passes through magnetic fields. Hartmann number can be expressed as:

$$H_a = B_0 D_h \sqrt{\frac{\sigma}{\mu}}$$

### 3.4 Numerical Simulation

The fluid flow domain has been discretised and the continuity and momentum equations are converted into the algebraic equations using  $2000 \times 20$  grids. The present study involves 40000 elements and 42021 nodes to conduct the numerical tests. The flow field under consideration is 20 mm long circular microchannel having diameter of 440  $\mu\text{m}$ . The actual numbers of meshes are finally selected on the basis of grid independence test for the final set of solution procedure. The total flow domain is discretized into non-overlapping rectangular mesh elements. For the solution of the governing equations, Semi-Implicit Method is used for pressure linked equations. This is a numerical method used to solve momentum equation. This algorithm is iterative in nature, where the boundary conditions are set up and the gradients of pressure and velocity are evaluated. The momentum equation in discretized form is used to compute the intermediate values of velocity field. Correction of mass fluxes at the faces and solution of the pressure correction equation yield cell values for the pressure correction. The pressure field and boundary pressure corrections are then updated for the each iteration thereby replacing the old values. For the numerical analysis, software package ANSYS Fluent Release 16.2 is used for this axisymmetric, double precision, pressure based, laminar flow through a circular microchannel. A program was written using user defined functions (UDF) to add Lorentz force as a source term in momentum equation. A sample program is given as follows. This program is written for conductivity  $0.02657 (\Omega\text{m})^{-1}$  and externally applied magnetic field of strength 0.3 T.

```
#include "udf.h"

DEFINE_SOURCE (x_mom_source,c, t)
{
    real source;
    float sigma=0.02657;
    int B=0.3;
    source =(sigma*B*B*(C_U(c,t)));
    return source;
}
```

### **3.4.1 Validity and Accuracy**

The validity of the current work has been compared with the research work of Barkhordari and Etemad [38], where the simulation has been done in no-slip flow and slip flow regimes for values of slip coefficients ranging from 0 to 0.2. The results of the present work have been validated with the results of Barkhordari for the velocity distribution of the fully developed power law fluid flow along the z-direction of the circular microchannel. The work justifies the result based on these values to validate the study and further improves upon it with the application of an externally applied magnetic field to present a novel approach towards the application in circular microchannel flow. In results and discussions section figures and tables are given to represent the data accuracy and validation process for the present work.

A two-step validation process has been adopted to test the accuracy of the results which involves MHD in the analysis. For the purpose, the results have been compared and validated with work of Hasan et. al. [61]. The results are validated for conducting fluid for no slip boundary condition at the wall.

While there have been previous studies on microchannels and non-Newtonian flow, but the combination of slip flow coupled with an externally applied magnetic field on a straight circular microchannel has not been taken up for study for applications pertaining to slip flow boundary conditions in combination with the magnetic field.

### **3.4.2 Stability and Convergence**

Numerical stability of the solution has been checked by the consistency of the finite difference equations derived from the governing equations of the present problem with help of the equations (8) to (16). Errors generated from the finite difference approximation are in decreasing order as the computation proceeds from the one iteration to the next. The convergence criteria for the present work have been set in the order of magnitude of  $1 \times 10^{-6}$ . On exceeding the value of  $10^{-6}$ , the iteration terminates to achieve the solution of the numerical procedure. The value of convergence criteria is same for the equation of continuity for both r and z coordinates. The present problem uses absolute convergence criteria for the solution as the flow is considered to be fully developed, steady and laminar.

### 3.5 Mesh Independence Test

Generally, for CFD analysis finer mesh generates better results. Finer mesh involves more nodes and elements which create more data points to capture finer contours of results. One can perform grid independence of mesh independence test to ascertain how much the outcomes depend on the mesh density.

For this work, grid independence studies were also made for three grid resolutions. From this study the final no of mesh resolution and nodes have been finalized to carry on the numerical simulation. Three mesh types were selected to check and confirm that the results do not depend on the mesh numbers. The results as obtained from this study are tabulated in Table 01.

Table 02 Result for Mesh Independence Study for  $\beta=0.2$

Flow behaviour index (n)	Velocity	Mesh Resolution		
		1800×10	2000×20	2200×30
n= 0.5	Slip Velocity	0.2021	0.2005	0.2001
	Centerline Velocity	1.535	1.53	1.531
n=1.0	Slip Velocity	0.21	0.202	0.2009
	Centerline Velocity	1.79	1.8	1.82
n=1.5	Slip Velocity	0.196	0.2	0.2003
	Centerline Velocity	1.97	1.96	1.97

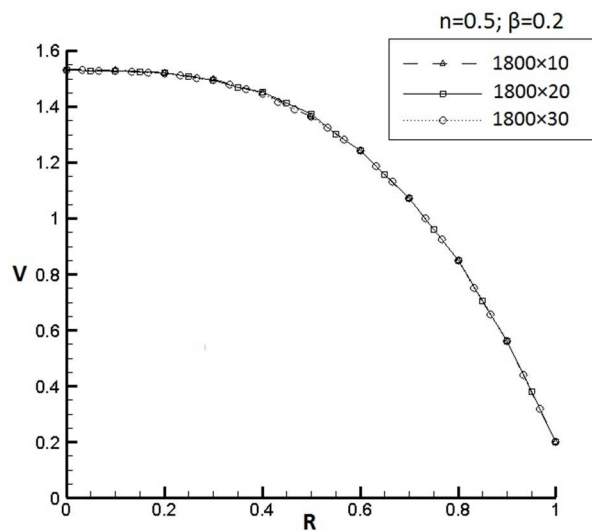


Fig. 08 Comparison of velocity profiles obtained from three different mesh resolutions for  $n=0.5$  and  $\beta=0.2$



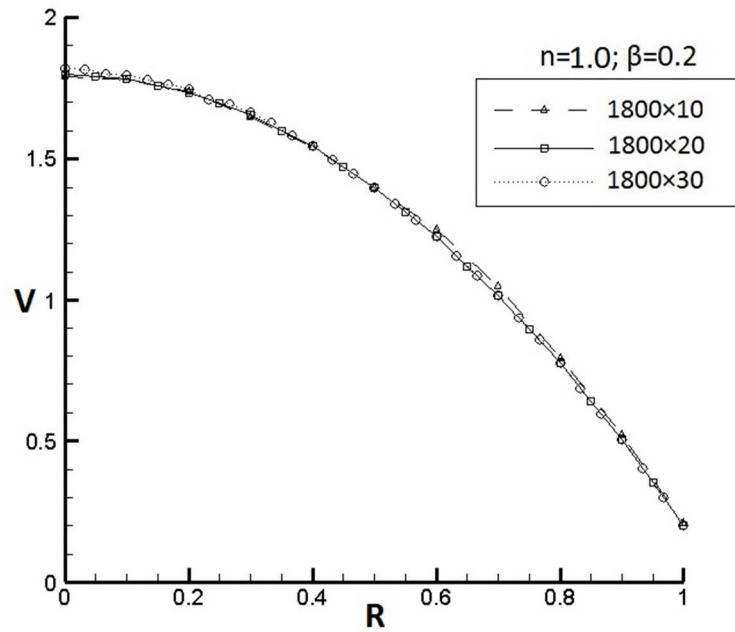


Fig. 09 Comparison of velocity profiles obtained from three different mesh resolutions for  $n=1.0$  and  $\beta=0.2$

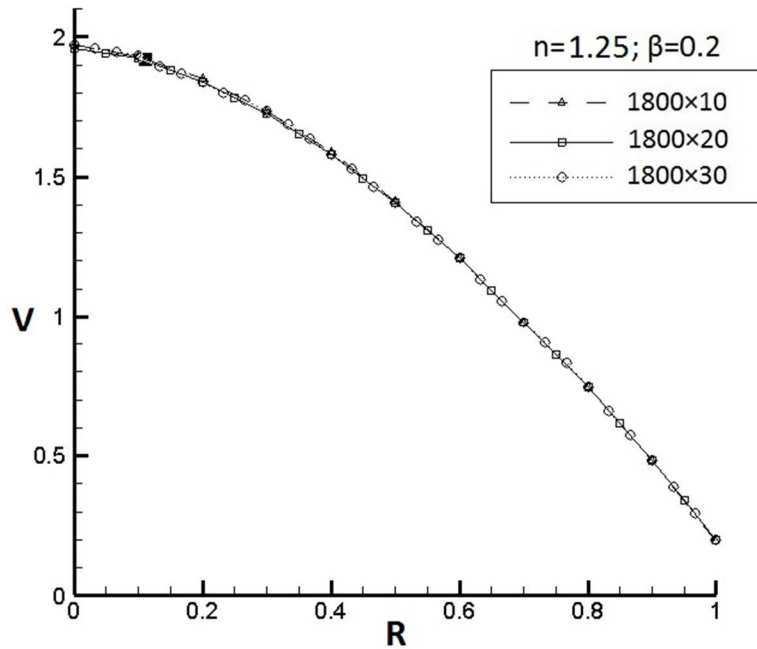


Fig. 10 Comparison of velocity profiles obtained from three different mesh resolutions for  $n=1.25$  and  $\beta=0.2$

A comparative study was made for the selection of the final mesh resolution from results as tabulated in Table 02 and depicted in Fig. 08, Fig. 09 and Fig. 10. It is observed that there is a little change in the results between these three tables and on the basis of this observation the mesh resolution of  $2000 \times 20$  have been chosen for further simulation and research work. Fig. 11 shows the final mesh, selected for the final calculations.

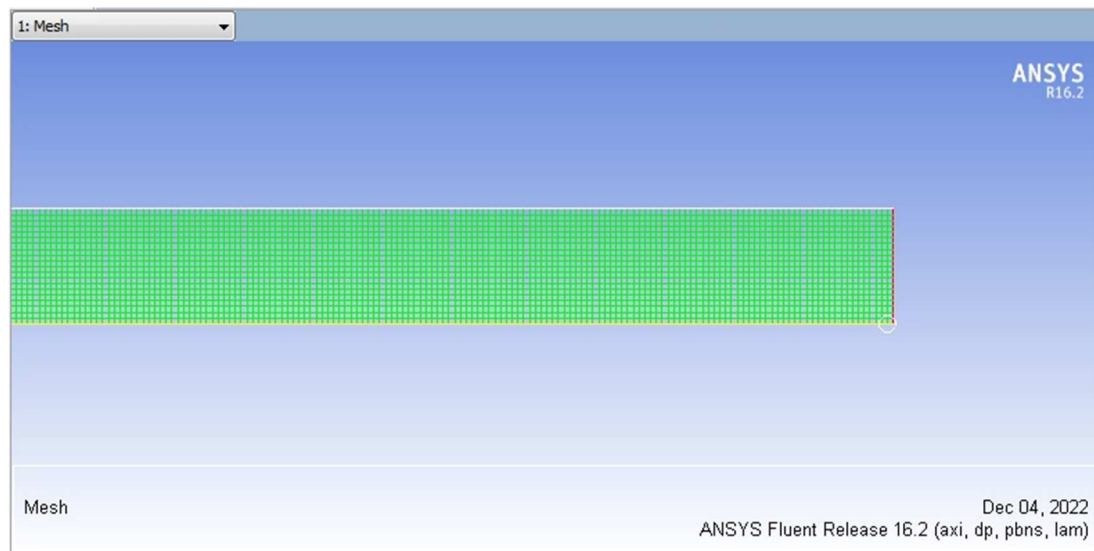


Fig. 11 Generated mesh showing finer distribution of mesh towards wall and centerline

## RESULTS AND DISCUSSION

---

In this section the results obtained from numerical analysis is summarized. There are two major section of this chapter. In first part the results of fully developed, hydrodynamic, steady flow of non-Newtonian fluids through microchannel is discussed. For the purpose, a validation has been done for slip induced non Newtonian fluid flow in microchannel. The results are validated with already available results of Barkhordari and Etemad [38].

In later part of the work, the microchannel flow is considered to be under the effect of magnetic field. In this section the results of slip induced non Newtonian fluid flow through circular microchannel with applied magnetic field is presented. For the purpose stated, a separate validation has been done again with the already available results of Hasan et.al. [61]. A two-step validation approach has been adopted to do the numerical analysis of slip induced non-Newtonian fluid flow through microchannels under the influence of externally applied magnetic field.

### 4.1 Slip Flow of Non Newtonian Fluids through Circular Microchannels

A study of non-Newtonian fluid flow through circular microchannel has been done numerically. Effect of slip flow at wall has been considered for fully developed, steady, laminar power law fluid. The work is carried out to analyze slip flow for different flow behavior index  $n=0.5$ ,  $n=1.0$  &  $n=1.5$  so as to make a comparison of flow characteristics between pseudoplastic ( $n=0.5$ ) and dilatant ( $n=1.5$ ) fluids with Newtonian fluid ( $n=1$ ) flow.

#### 4.1.1 Validation Slip Flow of Non Newtonian Fluids

In order to check the accuracy, the results of the present work have been validated with the results of Barkhoordari and Etemad [38] for the velocity distribution of the fully developed power law fluid along the radial direction of the circular microchannel. The result in Fig. 12 shows an excellent agreement with the available result for which  $n = 1.5$ ,  $Re = 100$ ,  $\beta = 0.2$  with no externally applied magnetic field. Besides this a comparison of maximum velocity attained along the centreline ( $V_{max}$ ) has been studied for slip and no slip conditions which is described in the Table 2. When the flow deviates from no slip to slip flow regime, the slip velocity of the flow

at the vicinity of the wall increases. This phenomenon forces the fluid to decrease the corresponding centreline velocity in order to maintain the requirement of mass conservation.

Table 03 Centreline velocities ( $V_{max}$ ) obtained for slip and no-slip conditions

n	No Slip Flow		Slip Flow			
	$\beta=0.0$		$\beta=0.1$		$\beta=0.2$	
	Barkhordari & Etemad	Present Study	Barkhordari & Etemad	Present Study	Barkhordari & Etemad	Present Study
0.5	1.67	1.66	1.59	1.57	1.53	1.5
1.0	2.00	1.99	1.89	1.9	1.8	1.8
1.25	2.11	2.07	2.00	1.96	1.88	1.86

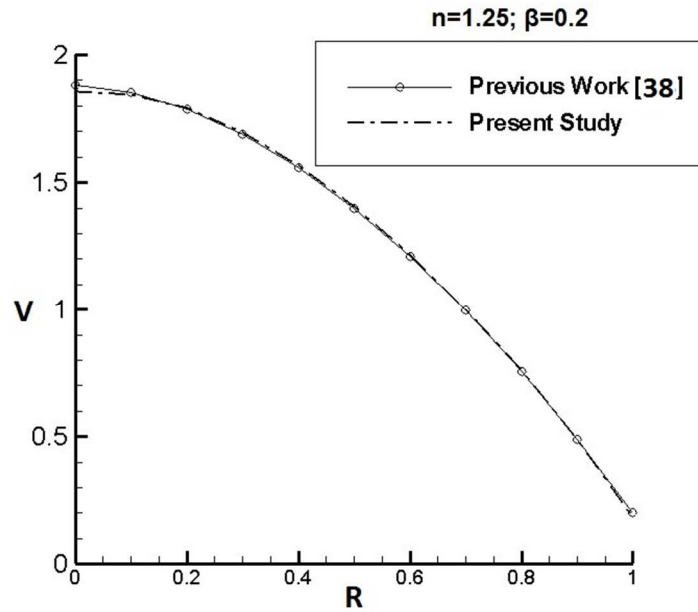


Fig. 12 Comparison of velocity profiles of present work and previous studies

Slip is a near wall phenomenon which can be quantified by the changing nature of the Re values as the microchannel flow shifts from no-slip to slip flow regime. Slip flow is more prominent in less wall shear stress which decreases the Re value when  $\beta$  increases (Table 04).

Table 04 f.Re values obtained from present work and previous studies for slip and no-slip conditions

n	No Slip Flow		Slip Flow			
	$\beta=0.0$		$\beta=0.1$		$\beta=0.2$	
	Barkhordari & Etemad	Present Study	Barkhordari & Etemad	Present Study	Barkhordari & Etemad	Present Study
0.5	6.32	6.31	5.97	5.80	5.63	5.72
1.0	16.00	15.95	14.31	14.12	12.72	12.20
1.25	25.24	25.10	21.95	22.25	18.95	20.26

#### 4.1.2 Results of Slip Driven Flow of Non Newtonian Fluids through Microchannels

To compare the effect of flow behavior index ( $n$ ) on fluid flow, Fig. 13 may be referred. It represents dimensionless velocity distribution for slip coefficient ( $\beta=0.1$ ). With the increment in 'n' velocity increases while velocity gradient decreases. The velocity profile for  $n<1$  (pseudoplastic fluids) is more uniform than that of dilatant fluids ( $n>1$ ), while the velocity profile of Newtonian fluid remains in between but the centerline velocity is closer to dilatant fluid. Fig 6 shows the velocity profile for  $n=0.5$  in which  $\beta$  varies from 0.1 to 0.3. With the increasing value of  $\beta$ , velocity at wall increases and corresponding centerline velocity decreases, which is in contrast to non-slip boundary condition, where velocity gradient decreases.

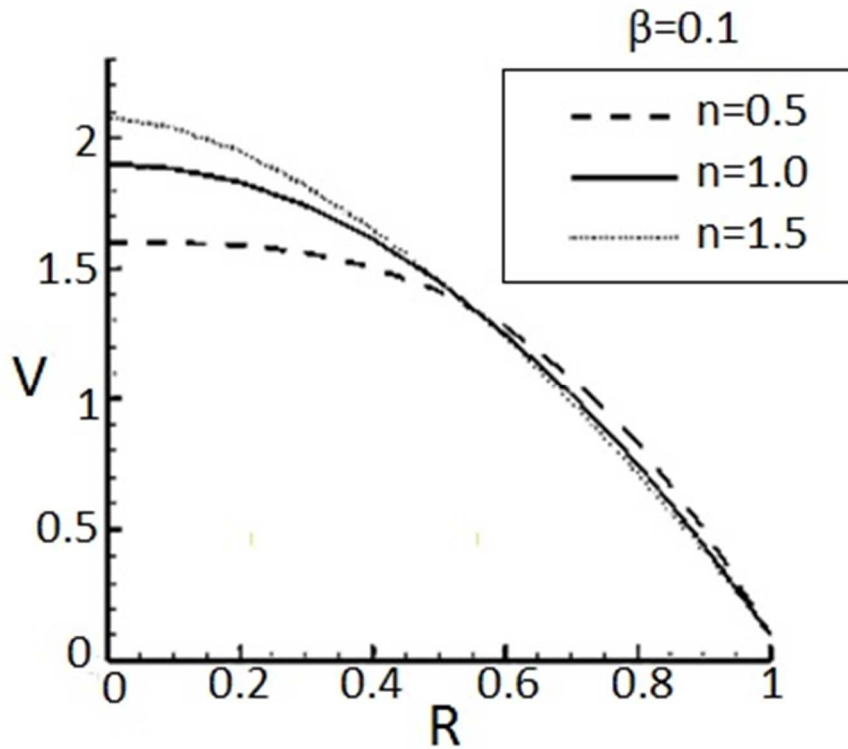


Fig. 13 Velocity profiles of slip flow through microchannel for different flow behaviour index

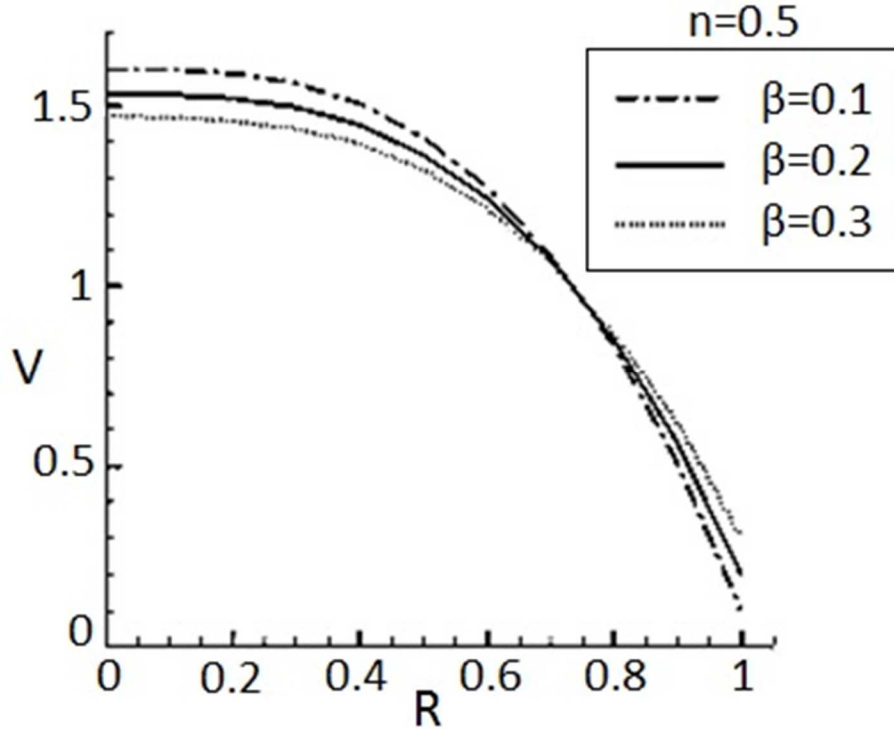


Fig. 14 Velocity profiles of slip flow through microchannel for different slip co-efficient

Fig. 15 shows the nature of variation of dimensionless slip length ( $L_s$ ) when compared to dimensionless slip coefficient ( $\beta$ ) for different values of 'n'. For a given value of 'n' the nature of variation in ' $L_s$ ' is increasing with increasing value of  $\beta$ . The variation in 'n' shows the similar nature between  $\beta$  and  $L_s$  except that the maximum value of slip length is observed in the increasing order (when 'n' varies). For instance, for the higher values of  $\beta$  slip length increases rapidly and the value of the same is 2.5 for  $n=1.5$  while it is 1.8 for  $n=0.5$ . Dilatant fluid always exhibits higher slip length in comparison to Newtonian and pseudoplastic fluids. Slip co-efficient  $\beta$  is having influencing control over centerline velocity or maximum velocity ( $V_{max}$ ). Fig. 16 depicts the decreasing tendency of  $V_{max}$  when  $\beta$  increases for different values of 'n'. Pseudoplastic fluids show lesser value of  $V_{max}$  when compared to Newtonian & dilatant fluids.  $V_{max}$  decreases linearly with the increasing value of  $\beta$ .

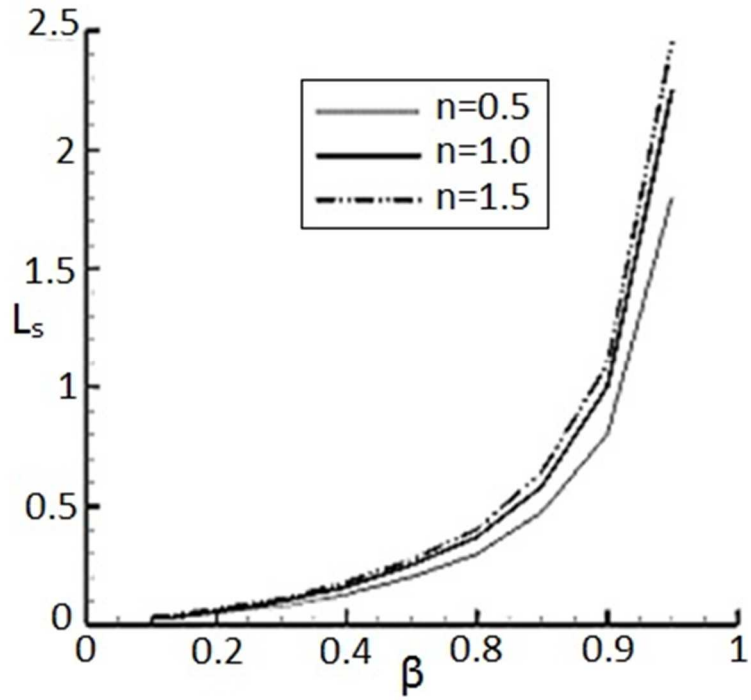


Fig. 15 Relation between slip length and slip coefficient.

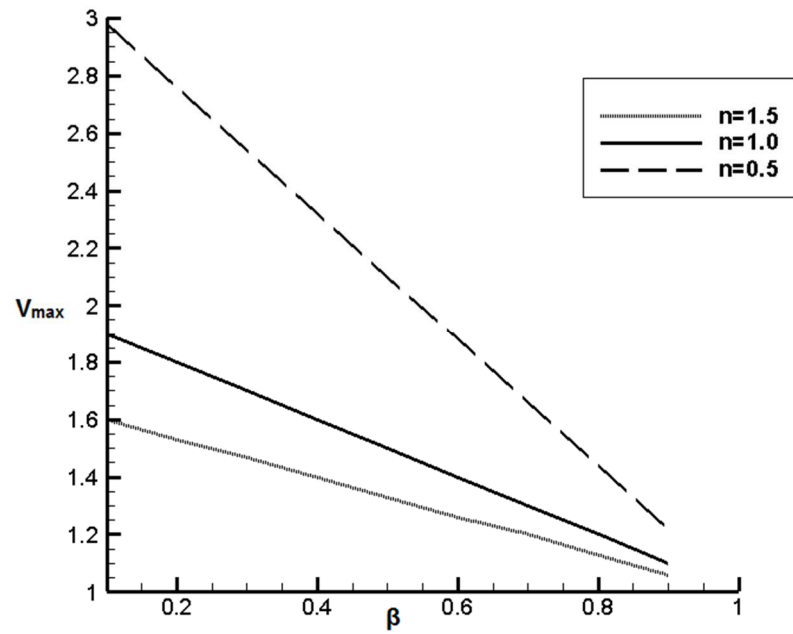


Fig. 16 Comparison of developed maximum velocity ( $V_{max}$ ) and Slip Coefficients ( $\beta$ )

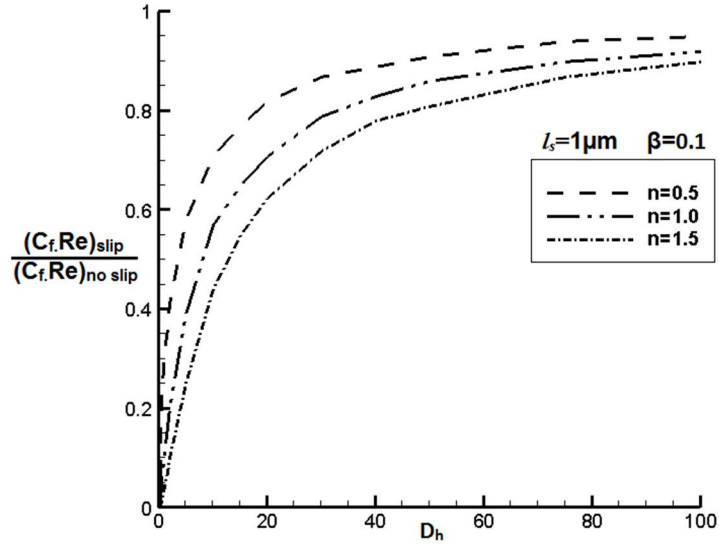


Fig. 17 Effect of hydraulic diameter ( $D_h$ ) on Poiseuille No. ( $C_f Re$ )

Hydraulic diameter ( $D_h$ ) affects wall friction no. ( $C_f Re$ ). This study reveals an increasing tendency of wall friction ratio between slip and no slip flow. When compared with hydraulic diameter for slip length ( $L_s$ ) = 1  $\mu m$  and  $\beta=0.1$  the nature of variation of wall friction is depicted in Fig. 17 which also represents the effect of flow behaviour index on wall friction number. As the value of  $n$  shifts from 0.5 to 1.5 the wall, friction ratio reduces. The rate of increment of friction value is higher for lower value of hydraulic diameter. As hydraulic diameter increases the rate of increment in friction decreases and becomes asymptotic after a particular value of  $D_h$ .

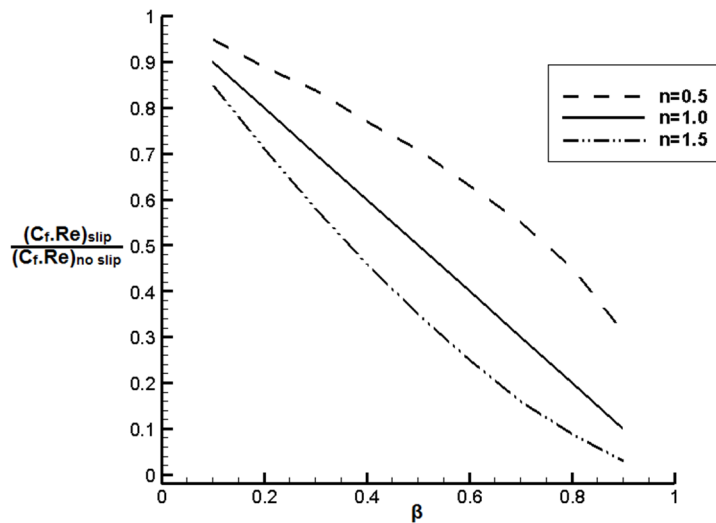


Fig. 18 Effect of slip coefficients on Poiseuille No.



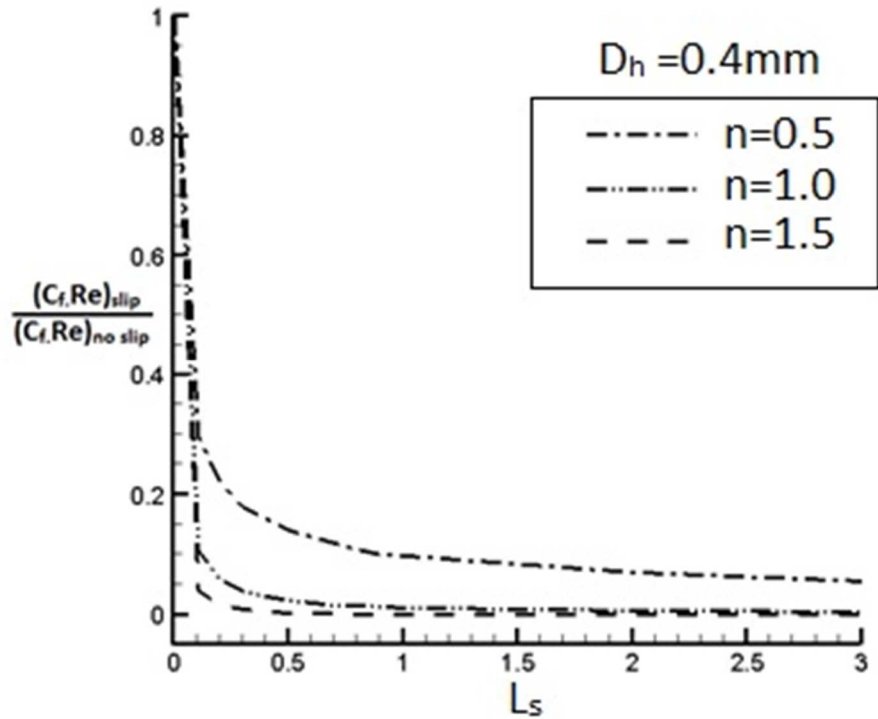


Fig. 19 Effect of slip length ( $l_s$ ) on  $C_f Re$  values

Slip flow is a near wall phenomena in which wall friction co-efficient or skin friction co-efficient plays a vital role to analyze the effect of different flow parameters on skin co-efficient Fig 18 has been drawn for the different value of 'n' . Newtonian fluids ( $n=1$ ) shows linear variation of friction values in decreasing manner when  $\beta$  is increased. Pseudoplastic and dilatant fluids shows non-linear variation which is shown in Fig 18. The curvature of the variation of pseudoplastic fluid is more than that of dilatant fluids and the curve of variation of dilatant is much closer to the linear variation which occurs for Newtonian fluids.

For the lower values of  $\beta$  the variation of skin co-efficient lies between 0.85 and 0.95. When  $\beta$  increases skin friction values decreases. But the difference in variation between pseudoplastic and dilatant fluid increases to the value of 0.2 to 0.6 for  $\beta=0.6$ .

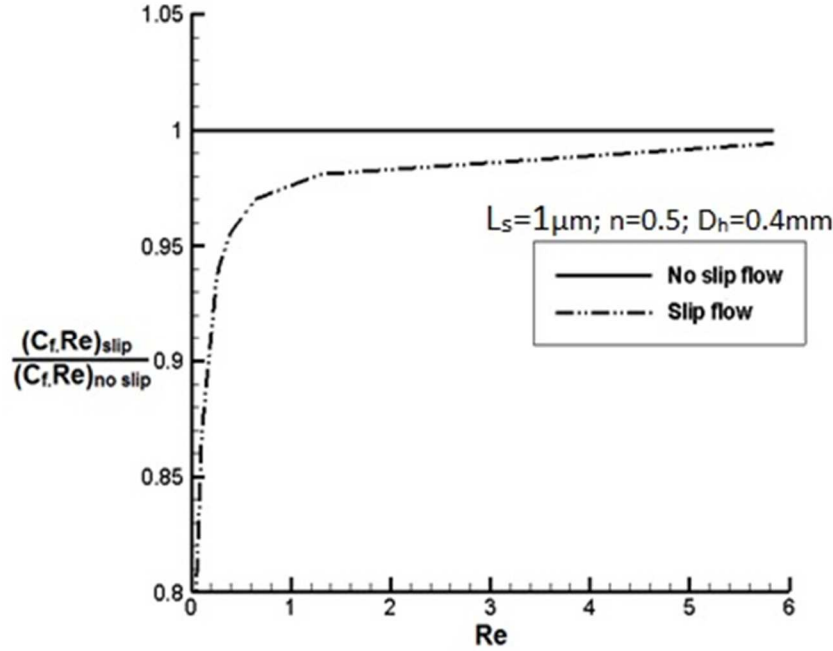


Fig. 20 Effect of Reynold's No. on  $C_f \cdot Re$  values

Fig. 19 shows the effect of slip length ( $L_s$ ) on skin co-efficient ratio of slip and no slip flow for hydraulic diameter of 0.4 mm and for different values of flow behaviour index. When slip length increases, initially friction values decreases rapidly and after the value of 0.5  $\mu\text{m}$  the curve becomes asymptotic in nature.

For dilatant and Newtonian fluids wall friction ratio becomes almost zero for the higher value of slip length. On the contrary, for pseudoplastic fluids when slip length is decreased, it shows the existence of higher friction values. For typical value of  $L_s = 0.5 \mu\text{m}$ , when friction value of pseudoplastic fluid is 1.8 in comparison to that of dilatant fluid which is having lesser value. The variation of wall friction is linear and in decreasing order when  $L_s$  increases from 0 to 0.1  $\mu\text{m}$  for all the values of  $n$ . A comparison between slip and no slip flow has been depicted in Fig. 20 for a fluid flow through a circular microchannel of 0.4 mm diameter. This figure is drawn for slip length  $L_s = 1 \mu\text{m}$ ,  $n = 0.5$  and  $D_h = 0.4 \text{ mm}$ . Fig 20 reveals an increasing tendency in skin friction ratio when Reynold's number is increased. For a very low Reynold's number, less than 5, wall friction has predominant role but opposite happens when Reynold's no. is more than 5 where the curve becomes asymptotic and reaches almost the value of friction co-efficient of no slip flow.

## 4.2 Results and Discussion of Slip Flow of Xanthan Solution in Formic Acid

The flow pattern of xanthan solution in formic acid under different intensities of externally applied magnetic field was studied for different slip coefficients ( $\beta$ ). The flow domain has been discretised which involves 40000 elements and 42021 nodes. The continuity and momentum equations were transformed into algebraic equations with the help of  $2000 \times 20$  grids. The actual numbers of meshes were selected on the basis of mesh independence of the final solution. Set of mesh sensitivity tests were done, before the final selection of mesh number in the flow field. Numerical simulation is done with the help of ANSYS release 16.2 software package. A sample velocity distribution across the radial direction is given. Slip velocity can be clearly seen at the vicinity of the wall.

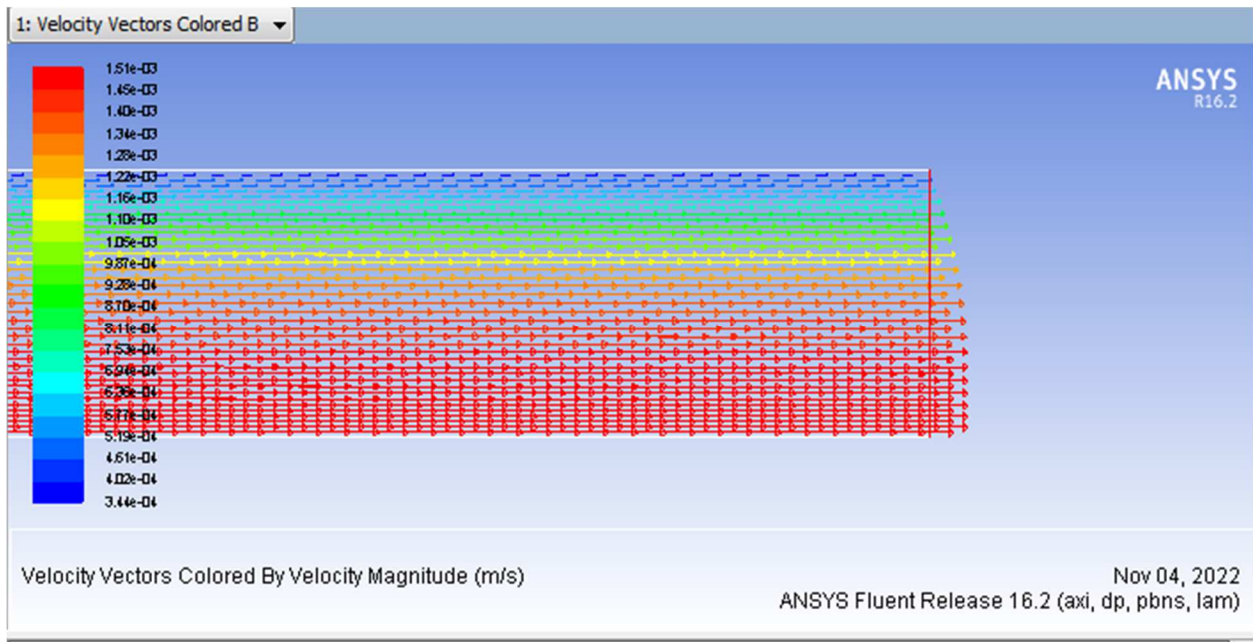


Fig. 21 Sample diagram of the distribution of velocity in the flow field

### 4.2.1 Validation of a conducting fluid under the influence of externally applied magnetic field

To test the accuracy of the result of MHD affected slip flow of non-Newtonian fluid through circular microchannel, a validation has been done with the available results of the work of Hasan et. al. [61]. Here the considered fluid is having fully developed, steady and laminar flow through a circular microchannel of diameter  $440 \mu\text{m}$ . In validation, centreline velocity ( $v_{\text{max}}$ ) is compared

with the outcomes of available results and a good agreement with the present numerical simulation can be seen in Fig. 22. This figure is drawn for different values of magnetic field lies in the range of 0.1 T to 1.0 T.

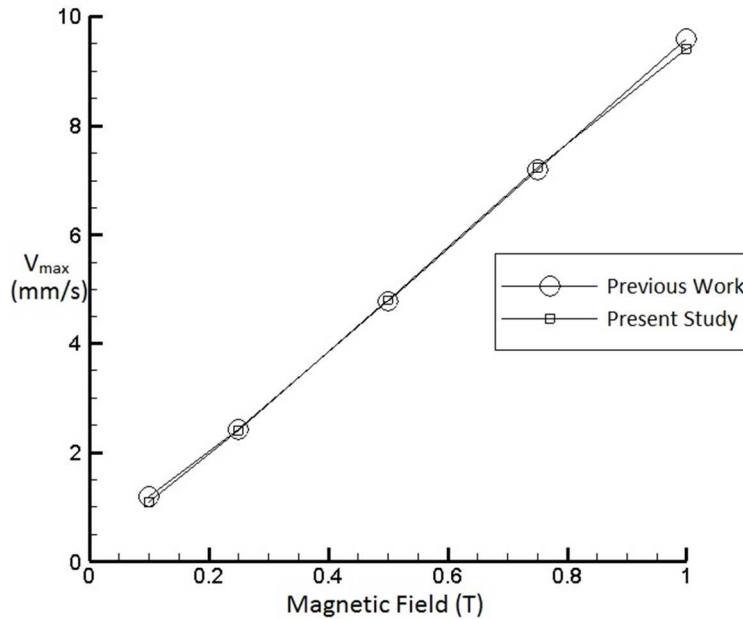


Fig. 22 Comparison of centreline velocity ( $v_{\max}$ ) obtained in present work and previous studies

#### 4.2.2 Results of Slip Flow of Xanthan Solution in Formic Acid

A comparison of different dimensionless velocity profiles are depicted in Fig. 23 for no slip ( $\beta=0.0$ ) and various slip flow when no magnetic field is applied and  $n = 0.761$ . It is observed that with the increasing value of  $\beta$  the velocity of the fluid at the vicinity of the wall increases and the centreline velocity decreases. In contrast to slip condition, for no slip condition, velocity gradient decreases at near wall region for higher values of  $\beta$ , in order to maintain the requirement of mass conservation a notable change in velocity profile is observed.

For the given fluid when magnetic fields of various intensities are applied on slip flow, then it is observed that with the increasing value of magnetic field the centreline velocity increases. In Fig. 24 a comparison is made between various dimensionless velocity profiles when  $\beta$  is left constant at 0.2. It is observed that the slip velocity also differs at the wall with the change of increasing intensities of externally applied magnetic field but that change is very insignificant.

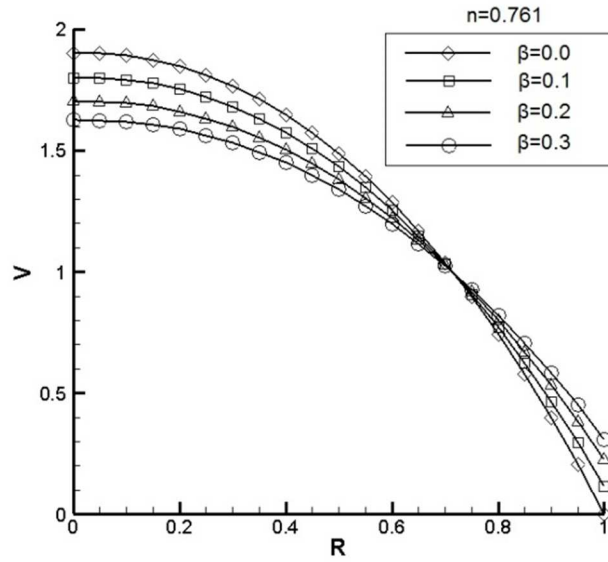


Fig. 23 Comparison of velocity profiles of slip and no slip flows for different values of slip coefficient ( $\beta$ ) when no magnetic field is applied

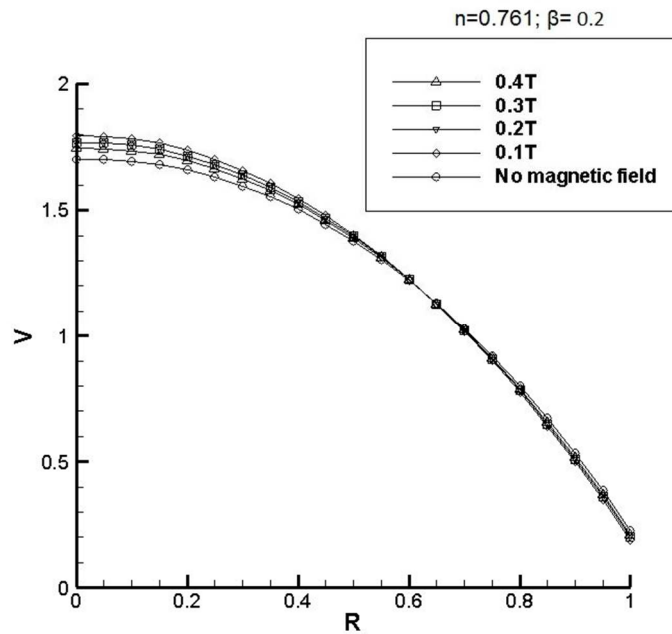


Fig. 24 Comparison of velocity profiles for different values of applied magnetic field ( $B_0$ ) when slip coefficient ( $\beta$ ) is 0.2

A comparison of different flow patterns due to different  $\beta$  values have been done by plotting the corresponding velocity profiles (Fig. 25) when exposed to externally applied magnetic field of

same intensity (0.3T). The plot shows a tendency that with the increase in  $\beta$ , slip velocity increases and corresponding centerline velocity decreases to maintain the momentum balance.

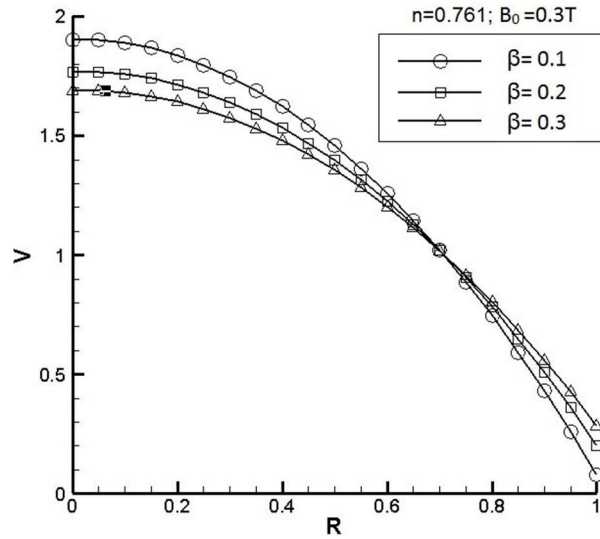


Fig. 25 Comparison of velocity profiles for the different values of  $\beta$  when applied magnetic field ( $B_0$ ) is held constant to 0.3T

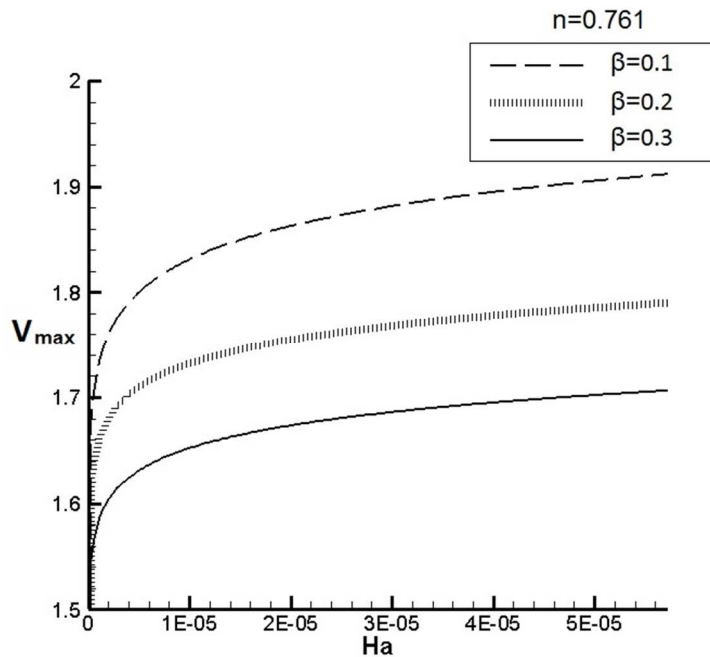


Fig. 26 Effect of Hartmann no ( $Ha$ ) on centreline velocity

Centerline velocity is affected by the applied magnetic field. Fig. 26 shows this tendency. With the increment in Hartmann number ( $Ha$ ), electromagnetic force becomes predominant in comparison to viscous force which increases the centerline velocity of the fluid flow having different slip coefficients. In contrast to the centerline velocities, slip velocity near wall shows opposite tendency. When  $Ha$  increases, slip velocity decreases rapidly to certain value and at the later stage this influence becomes less significant. This comparison shows centerline velocity is much more affected by magnetic field in comparison to slip velocity (Fig. 27).

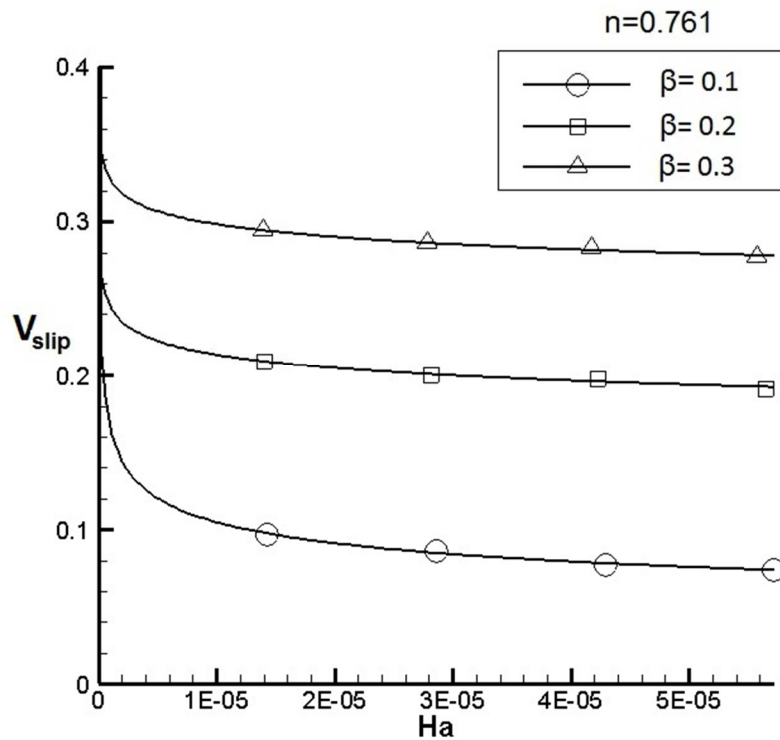


Fig. 27 Effect of Hartmann no ( $Ha$ ) on slip velocity

When comparing the relation between  $\beta$  and  $Ha$ , the result reveals that, with the increasing value of  $Ha$ , slip coefficient decreases. This tendency is much prominent in the region where  $\beta$  is less. With the increment of  $\beta$ , this tendency decreases (Fig. 28).

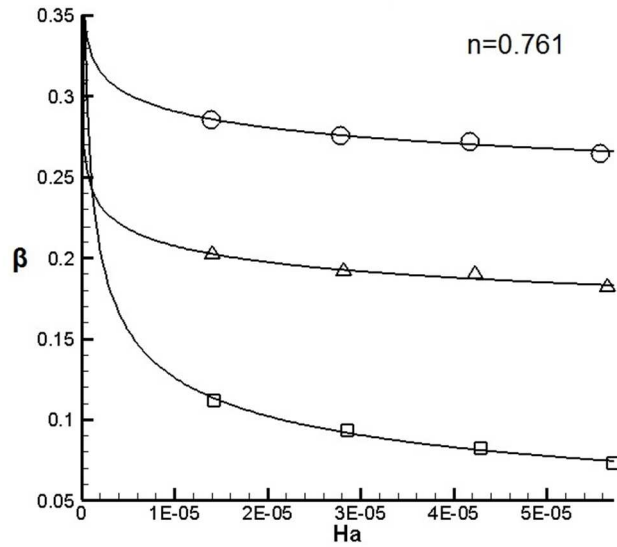


Fig. 28 Effect of Hartmann No (Ha) on Slip co-efficient ( $\beta$ )

Fig. 29 depicts a graphical representation of centerline velocity for different  $\beta$  when they are exposed to a same  $B_0 = 0.4T$ . This diagram shows the gradual development of the flow along the microchannel and at the 20% microchannel length flow develops to be a fully developed flow on which the electromagnetic force is applied. For the given conditions, the fluid flow having less  $\beta$  exhibits maximum centerline velocity.

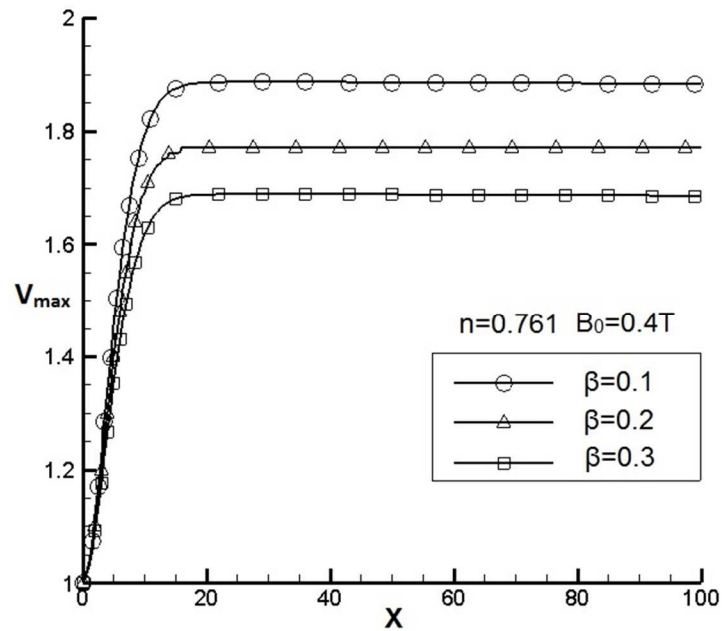


Fig. 29 Comparison of  $V_{max}$  v/s  $X$  for  $B_0=0.4T$  for the different values of  $\beta$



In Fig. 30 a comparison of  $f.Re$  values for the different  $\beta$  to find out the fact that, when  $\beta$  is less  $f.Re$  becomes more which makes the slip velocity less. But opposite happens with the increase in  $\beta$  and consequently  $f.Re$  decreases and slip velocity increases.

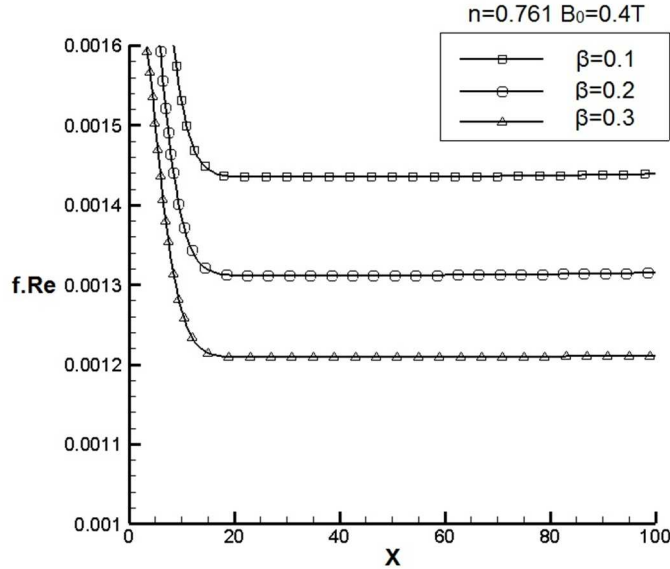


Fig. 30 Comparison of  $f.Re$  v/s  $X$  for  $B_0=0.4T$  for the different values of  $\beta$

A comparison in the values of  $V_{max}$  and  $V_{slip}$  is drawn in Table 5 and Table 6 for the different values of  $\beta$  and applied magnetic field. When externally applied magnetic field is acted on the flow, slip flow decreases and corresponding centerline velocity increases in each case to maintain the momentum balance.

Table 5 Comparison of the developed  $V_{max}$  for different MHD

Varying Magnetic Field intensities ( $B_0$ )	Varying Slip Coefficient ( $\beta$ )		
	0.1	0.2	0.3
0	1.80	1.70	1.62
0.1T	1.84	1.75	1.66
0.2T	1.88	1.76	1.68
0.3T	1.90	1.77	1.69
0.4T	1.91	1.79	1.71
Relative difference % = $\frac{(U_{max})_{B_0=0.4T} - (U_{max})_{B_0=0.0T}}{(U_{max})_{B_0=0.0T}} \times 100$	6.1	5.9	5.6

Table 6 Comparison of the developed  $V_{slip}$  for different MHD

Varying Magnetic Field intensities ( $B_0$ )	Varying Slip Coefficient ( $\beta$ )		
	0.1	0.2	0.3
0	0.110	0.225	0.308
0.1T	0.098	0.209	0.294
0.2T	0.086	0.200	0.286
0.3T	0.077	0.198	0.283
0.4T	0.074	0.191	0.277
Relative difference % = $\frac{(U_{slip})_{B_0=0.4T} - (U_{slip})_{B_0=0.0T}}{(U_{slip})_{B_0=0.0T}} \times 100$	32.73	15.11	10.06

When Xanthan is mixed with different concentrations in formic acid then the values of flow behaviour index and consistency index changes along with the conductivity. This is shown in Table 01. A comparison of velocity profile is done to understand the effect of increasing concentration and conductivity on the fluid flow when a constant magnetic field of 0.1T is applied for three different concentrations. It is observed that when concentration is increased, centerline velocity decreases due to the application of magnetic field and the same also happens for slip velocity also. This is due to the fact of increasing value of electrical conductivity of the solution when the concentration increases.

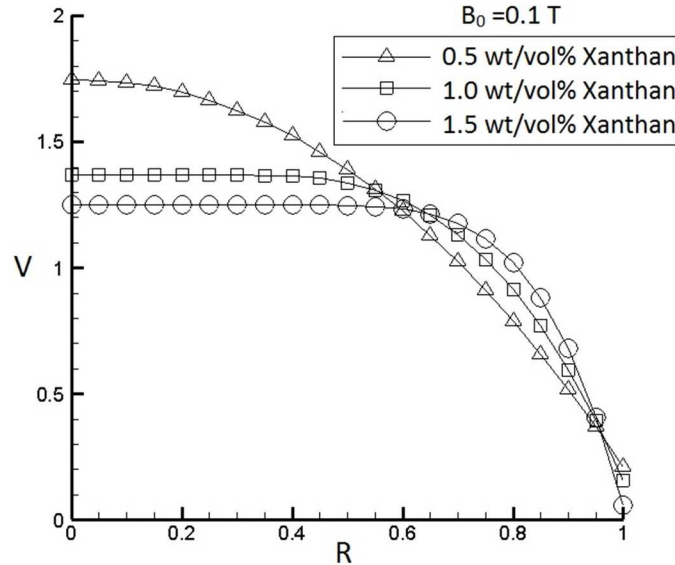


Fig. 31 Velocity profiles of Xanthan solutions of different concentrations

## CONCLUSIONS

---

This analysis and numerical study of slip flow of non-Newtonian fluids through circular microchannels reveal various observations among which following are the salient points to note. On the basis of the present work, the conclusions are as follows:

### 5.1 Slip flow of non-Newtonian fluids through microchannels

- i. The velocity profile of slip flow shows that pseudoplastic fluids have higher centerline velocity and discharge than that of dilatant fluid when they are exposed to same slip coefficient  $\beta$ .
- ii. If slip coefficient decreases for a constant flow behaviour index then centerline velocities increases and slip velocity decreases. Slip coefficient ( $\beta$ ) affects the flow parameters like dimensionless slip-length, centerline velocity and wall friction coefficient. With the increasing tendency of  $\beta$ , dimensionless slip length increases and consequently centerline velocity decreases linearly. The maximum variation in these parameters can be seen for pseudoplastic fluids. For dilatant fluid the nature of effect remains similar but less predominant.
- iii. When  $\beta$  increases, the effect of skin co-efficient in wall decreases gradually. This compared to Newtonian fluids, the same remains linear.
- iv. When hydraulic diameter increases then wall friction effect increases and after a certain value the same becomes asymptotic. The opposite nature of skin co-efficient effect can be seen when slip length is increased. This nature of variation is most predominant in pseudoplastic fluids which increase with the decrement of flow behaviour index. For a very low Reynold's no (typically  $Re < 5$ ) skin co-efficient factor has predominant role to play.

### 5.2 Slip Flow of Xanthan solution through microchannel under the influence of externally applied magnetic field

The present work is dedicated to find out the effect of externally applied magnetic field through straight microchannel having circular cross section. Numerical analysis is done to study the hydrodynamic, fully

developed, steady, laminar slip flow with different values of applied magnetic field for a typical non-Newtonian fluid (Xanthan solution). After the completion, following are few notable conclusions that are drawn from the present work.

- i. Externally applied magnetic field increases the centerline velocity in slip flow of a non-Newtonian fluid and corresponding slip velocity decreases and consequently slips coefficient decreases.
- ii. The effect of magnetic field is much prominent on slip velocities than that of centerline velocities.
- iii. Externally applied magnetic field also affects centerline velocities but the intensity is much less than that of slip velocity.
- iv. When slip co-efficient ( $\beta$ ) increases wall friction decreases for different values of  $\beta$ .
- v. With the increment of Hartmann number ( $Ha$ ), slip co-efficient decreases and the effect of slip diminishes towards no slip regime.
- vi. Due to the Lorentz force of electromagnetic origin, axial velocity increases which introduce extra flow through microchannel.

### **5.3 Future scope of work**

Numerical analysis of the flow of Xanthan solution in Formic acid through microchannels reveals the results of slip flow of non-Newtonian fluid under the influence of externally applied magnetic field. Findings from present study can be used for better design of microchannel flow in MEMS. There remains an ample scope of research works that can be extended in the field of fluid mechanics, heat transfer, bio fluid analysis and MEMS. Following are few suggestive directions for scope of future works.

- i. Flow optimization can be done by considering various cross sections for the slip flow of non-Newtonian fluids.
- ii. Heat transfer analysis in connection to the flow field under the influence of various intensities of magnetic field can be done.
- iii. Research works can be conducted to analyze the effect of slip flow, MHD etc. on various bio fluids like blood, proteins etc.

## Appendix A

<b>A.1 Data sheet showing the results of numerical analysis of 0.5wt/vol% Xanthan solution in formic acid</b>									
$\rho$	1225	Kg/m <sup>3</sup>	L	0.02	m	$u_e$	0.01	m/s	
n	0.761		$D_h$	$0.4 \times 10^{-3}$	m	conductivity	0.01343	( $\Omega m$ ) <sup>-1</sup>	
K	0.214		$r_0$	0.0002	m				
$\Delta p$	$\dot{\gamma}$	$\tau_w$	$\mu_{eff}$	$u_{max}$	$u_{slip}$	$u_{avg}$	$\beta$	$B_0$	Remarks
4300	427.23	21.5	0.1028	0.01902	0.0000188	0.0102	0.00184	0	
3900	375.79	19.5	0.1052	0.01801	0.00114	0.01021	0.11165	0	
				0.01848	0.00097	0.01021	0.111656	0.1T	
				0.01877	0.00086	0.010384	0.093413	0.2T	
				0.01902	0.00077	0.010489	0.08199	0.3T	
				0.01910	0.00074	0.010582	0.072766	0.4T	
3500	325.98	17.496	0.10789	0.01701	0.00225	0.010185	0.220903	0	
				0.01744	0.00209	0.010343	0.202075	0.1T	
				0.01768	0.00200	0.01043	0.191753	0.2T	
				0.01774	0.00198	0.010453	0.189417	0.3T	
				0.01794	0.00191	0.010528	0.181416	0.4T	
3200	289.77	15.99	0.1103	0.01626	0.00308	0.010166	0.30297	0	
				0.01663	0.00294	0.0103	0.285431	0.1T	
				0.01685	0.00286	0.010382	0.27549	0.2T	
				0.01690	0.00283	0.010395	0.272259	0.3T	
				0.01710	0.00277	0.010474	0.264457	0.4T	

<b>A.2 Data sheet showing the results of numerical analysis of 1.0 wt/vol% Xanthan solution in formic acid</b>									
$\rho$	1230	Kg/m <sup>3</sup>	L	0.02	m	$u_e$	0.01	m/s	
n	0.473		$D_h$	$0.4 \times 10^{-3}$	m	conductivity	0.02657	( $\Omega m$ ) <sup>-1</sup>	
K	2.274		$r_0$	0.0002	m				
$\Delta p$	$\dot{\gamma}$	$\tau_w$	$\mu_{eff}$	$u_{max}$	$u_{slip}$	$u_{avg}$	$\beta$	$B_0$	remarks
6800	304.29	33.99	0.1117	0.01418	$7.98 \times 10^{-5}$	$8.67 \times 10^{-3}$	0.0092	0	
6500	276.6	32.49	0.1175	0.01386	0.000963	0.008827	0.109097	0	
				0.01386	0.000963	0.008827	0.109097	0.1T	
				0.01392	0.000877	0.00883	0.09932	0.2T	
				0.01394	0.000850	0.008832	0.096244	0.3T	
				0.01402	0.000743	0.008839	0.084062	0.4T	
6200	250.31	30.99	0.1238	0.01354	0.00177	0.008947	0.197835	0	
				0.01354	0.00177	0.008947	0.197835	0.1T	
				0.01358	0.001704	0.008945	0.190488	0.2T	
				0.01360	0.001679	0.008948	0.187642	0.3T	
				0.01361	0.001661	0.008947	0.185649	0.4T	
5850	221.38	29.24	0.1321	0.01310	0.00276	0.009065	0.304472	0	
				0.01311	0.00275	0.009067	0.303295	0.1T	
				0.01314	0.00270	0.009066	0.297821	0.2T	
				0.01315	0.00268	0.009064	0.29567	0.3T	
				0.01322	0.00259	0.009072	0.285503	0.4T	

**A.3 Data sheet showing the results of numerical analysis of 1.5wt/vol%  
Xanthan solution in formic acid**

$\rho$	1235	Kg/m <sup>3</sup>	L	0.02	m	$u_e$	0.01	m/s	
n	0.317		$D_h$	$0.4 \times 10^{-3}$	m	conductivity	0.03567	( $\Omega m$ ) <sup>-1</sup>	
K	10.617		$r_0$	0.0002	m				
<b><math>\Delta p</math></b>	<b><math>\dot{\gamma}</math></b>	<b><math>\tau_w</math></b>	<b><math>\mu_{eff}</math></b>	<b><math>u_{max}</math></b>	<b><math>u_{slip}</math></b>	<b><math>u_{avg}</math></b>	<b><math>\beta</math></b>	<b><math>B_0</math></b>	<b>Remarks</b>
15000	477.270	75.019	0.1572	0.01255	0.000183	0.00854	0.02	0	
14500	428.875	72.52	0.1691	0.01226	0.001183	0.00867	0.136	0.0 T	
				0.01273	0.000269	0.00869	0.031	0.1 T	
				0.01274	0.000177	0.00866	0.020	0.2 T	
				0.01275	0.000126	0.00865	0.014	0.3 T	
				0.01276	0.000096	0.00865	0.011	0.4 T	
14200	401.499	71.018	0.1769	0.01219	0.001691	0.00878	0.19	0.0 T	
				0.01252	0.000595	0.00852	0.069	0.1 T	
				0.01252	0.000568	0.00864	0.066	0.2 T	
				0.01253	0.000522	0.00863	0.060	0.3 T	
				0.01254	0.000435	0.00861	0.050	0.4 T	
14000	383.93	70.018	0.2606	0.012	0.00293	0.0091	0.32	0.0 T	
				0.01216	0.002431	0.0090	0.27	0.1 T	
				0.01223	0.002153	0.00896	0.24	0.2 T	
				0.01223	0.00213	0.00895	0.238	0.3 T	
				0.01224	0.00210	0.00895	0.234	0.4 T	

## REFERENCES

- [1] Gad-el-Hak M., The Fluid Mechanics of Microdevices - The Freeman Scholar Lecture, *Journal of Fluids Engineering*, 1999, Vol. 121, pp. 5-33.
- [2] Bird R.B., Armstrong R.C. and Hassager O., *Dynamics of Polymeric Liquids*, John Wiley & Sons, 1987, pp. 3-294.
- [3] Chhabra R.P. and Richardson J.F., *Non-Newtonian Flow and Applied Rheology Engineering Applications*, Butterworth-Heinemann, 2008, pp. 1-205.
- [4] Anderson J.D., Jr., *Computational Fluid Dynamics: The Basics with Applications*, McGraw-Hill, Inc., 1995, pp. 3-446.
- [5] Patankar S.V., *Numerical Heat Transfer and Fluid Flow*, McGraw-Hill Book Company, 1980, pp. 11-150.
- [6] Brochard F. and de Gennes P.G., Shear-Dependent Slippage at a Polymer/Solid Interface, *Langmuir*, Vol. 8, 1992, pp. 3033-3037.
- [7] de Gennes P.G., On Fluid/Wall Slippage, *Langmuir*, Vol. 18, 2002, pp. 3413-3413.
- [8] Bocquet L. and Barrat J.L., Flow Boundary Conditions from Nano to Micro-scales, *Soft Matter*, Vol. 3, 2007, pp. 685-693.
- [9] Brenner H., Beyond the No-Slip Boundary Condition. *American Physical Society Physical Review*, Vol. 84, Issue 4, 2011, pp. 046309/1-8.
- [10] Pismen L.M. and Rubenstein B.Y., Kinetic Slip Condition, Van Der Waals Forces, and Dynamic Contact Angle, *Langmuir*, Vol. 17, No. 17, 2001, pp. 5265-5270.
- [11] Hetsroni G., Mosyak A., Pogrebnyak E. and Yarin L.P., Fluid in Micro-Channels, *International Journal of Heat and Mass Transfer*, Vol. 48, 2005, pp. 1982-1998.
- [12] Hoseinzadeh S., Heyns P.S., Chamkha A.J. and Shirkhani A., Thermal Analysis of Porous Fins Enclosure with the Comparison of Analytical and Numerical Methods, *Journal of Thermal Analysis and Calorimetry*, Vol. 138, 2019, pp. 727-735.
- [13] Sarabandi A.H., Moghadam A.J., Thermal Analysis of Power-Law Fluid Flow in a Circular Microchannel, *Journal of Heat Transfer*, Vol. 139, 2017, pp. 032401/1-14.
- [14] Avramenko A.A., Dmitrenko N.P., Shevchuk I.V., *Journal of Thermal Analysis and Calorimetry*, Vol. 144, 2020, pp. 955-961.
- [15] Chakraborty S., Dynamics of Capillary Flow of Blood into a Microfluidic Channel, *Lab Chip*, Vol. 5, 2005, pp. 421-430.

- [16] Crochet M.J. and Walters K., Numerical Methods in Non-Newtonian Fluid Mechanics, Annual Reviews Fluid Mechanics, Vol. 15, 1983, pp. 241-260.
- [17] Thompson P.A. and Robbins M.O., Physical Review A, Vol. 41, No. 12, 1990, pp. 6830-6837.
- [18] Thompson P.A. and Troian S.M., A General Boundary Condition for Liquid Flow at Solid Surfaces, Nature, Vol. 389, 1997, pp. 360-362.
- [19] Ameen T.A., Wang X., Barron R.F. and Warrington R.O., Jr., Laminar Forced Convection in a Circular Tube with Constant Heat Flux and Slip Flow, Microscale Thermophysical Engineering, Vol. 1, 1997, pp. 303-320.
- [20] Liu D. and Garimella S.V., Investigation of Liquid Flow in Microchannels, CTREC Research Publications, Paper 295, 2004, pp. 1-34.
- [21] Tretheway D.C. and Meinhart C.D., Apparent Fluid Slip at Hydrophobic Microchannel Walls, Physics of Fluids, Vol. 14, No. 3, 2002, pp. L9-L12.
- [22] You X.Y., Zheng J.R. and Jing Q., Effects of Boundary Slip and Apparent Viscosity on the Stability of Microchannel Flow, ForschIngenieurwes, Vol. 71, 2007, pp. 99-106.
- [23] Kashaninejad N., Chan W.K. and Nguyen N.T., Analytical Modeling of Slip Flow in Parallel-plate Microchannels, Micro and Nanosystems, Vol. 5, No.4, 2013, pp. 245-252.
- [24] Tang G.H., Ye P.X. and Tao W.Q., Electroviscous Effect on Non-Newtonian Fluid Flow in Microchannels, Journal of Non-Newtonian Fluid Mechanics, Vol. 165, 2010, pp. 435-440.
- [25] Avsec J., Vrtič P., Naterer G, Nanofluid and ferrofluid slip flow in rectangular and circular microchannels and minichannels , Przegląd Elektrotechniczny (Electrical Review), Vol. 87 No. 3, 2011, pp. 5-8.
- [26] Shakir A.M., Mohammed A.K. and Hasan M.I., Numerical Investigation of Counter Flow Microchannel Heat Exchanger With Slip Flow Heat Transfer, International Journal of Thermal Sciences, Vol. 50, 2011, pp. 2132-2140.
- [27] Yazdi M.H., Hashim I., Fudholi A., Ooshaksaraei P. and Sopian K., Entropy Generation Analysis of Power-Law Non-Newtonian Fluid Flow Caused by Micropatterned Moving Surface, Mathematical Problems in Engineering, Vol. 2014, 2014, pp. 1-16.
- [28] Bushehri M.R.S., Ramin H. and Salimpour M.R., A New Coupling Method for Slip-Flow and Conjugate Heat Transfer in a Parallel Plate Micro Heat Sink, International Journal of Thermal Sciences, Vol. 89, 2015, pp. 174-184.



- [29] Kountouriotis Z., Philippou M. and Georgiou G.C., Development Lengths in Newtonian Poiseuille Flows with Wall Slip, *Applied Mathematics and Computation*, Vol. 291, 2016, pp. 98-114.
- [30] Ferrás L.L., Afonso A.M., Alves M.A., Nóbrega J.M., Carneiro O.S. and Pinho F.T., Slip Flows of Newtonian and Viscoelastic Fluids in a 4:1 Contraction, *Journal of Non-Newtonian Fluid Mechanics*, Vol. 214, 2014, pp. 28-37.
- [31] Ashrafi T.G., Hoseinzadeh S., Sohani A. and Shahverdi M.H., *Mathematical Methods in the Applied Sciences*, Vol. 44, Issue 8, 2021, pp. 7017-7030.
- [32] Nishad C. S., Chandra A. and Raja Sekhar G.P., Flows in slip-patterned micro-channels using boundary element method, *Engineering Analysis with Boundary Elements*, Vol. 73, 2016, pp. 95-102.
- [33] Shojaeian M. and Dibaji S.A.R., Three-Dimensional Numerical Simulation of the Slip Flow Through Triangular Microchannels, *International Communications in Heat and Mass Transfer*, Vol. 37, 2010, pp. 324-329.
- [34] Nagayama G., Matsumoto T., Fukushima K. and Tsuruta T., Scale Effect of Slip Boundary Condition at Solid–Liquid Interface, *Scientific Reports*, Vol. 7, 2017, pp. 1-8.
- [35] Öztürk A. and Kahveci K., Slip Flow of Nanofluids between Parallel Plates Heated with a Constant Heat Flux, *Strojniški vestnik - Journal of Mechanical Engineering*, Vol. 62, Issue 9, 2016, pp. 511-520.
- [36] Zhang X., He F., Hao P., Gao Y., Sun L., Wang X. and Jin X., Characteristics of Liquid Flow in Microchannels at very Low Reynolds Number, *Chemical Engineering & Technology*, Vol. 39, Issue 8, pp. 1425-1430.
- [37] Yang X., Weldetsadik N.T., Hayat Z., Fu T., Jiang S., Zhu C. and Ma Y., Pressure Drop of Single Phase Flow in Microchannels and its Application in Characterizing the Apparent Rheological Property of Fluids, *Microfluidics and Nanofluidics*, Vol. 23, No. 75, 2019, pp. 1-9.
- [38] Barkhordari M. and Etemad S. Gh., Numerical Study of Slip Flow Heat Transfer of Non-Newtonian Fluids in Circular Microchannels, *International Journal of Heat and Fluid Flow*, Vol. 28, 2007, pp. 1027-1033.
- [39] Chakraborty S., Non-Newtonian Fluids in Microchannel. In: Li, D. (eds) *Encyclopedia of Microfluidics and Nanofluidics*, Springer, 2008, pp. 1471-1480.
- [40] Anna S.L., Non-Newtonian Fluids in Microfluidics. In: Li, D. (eds) *Encyclopedia of Microfluidics and Nanofluidics*, Springer, pp. 1480-1488.

- [41] Etemad S. Gh., Laminar Heat Transfer to Viscous Non-Newtonian Fluids in Non-Circular Ducts, Ph.D Thesis, Department of Chemical Engineering, McGill University, 1995, pp. 1-175.
- [42] Muzychka Y.S. and Edge J., Laminar Non-Newtonian Fluid Flow in Noncircular Ducts and Microchannels, *Journal of Fluids Engineering*, Vol. 130, 2008, pp. 111201/1-7.
- [43] Niu j., Fu C. and Tan W., Slip-Flow and Heat Transfer of a Non-Newtonian Nanofluid in a Microtube, *PLoS One*, Vol. 7, Issue 5, 2012, pp. 1-9.
- [44] Mansour M.H., Kawahara A. and Sadatomi M., Experimental Investigation of Gas–Non-Newtonian Liquid Two-Phase Flows from T-Junction Mixer in Rectangular Microchannel, *International Journal of Multiphase Flow*, Vol. 72, 2015, pp. 263-274.
- [45] Sajadifar S.A., Karimipour A. and Toghraie D., Fluid Flow and Heat Transfer of Non-Newtonian Nanofluid in a Microtube Considering Slip Velocity and Temperature Jump Boundary Conditions, *European Journal of Mechanics B/Fluids*, Vol. 61, 2017, pp. 25-32.
- [46] Sarabandi A.H. and Moghadam A.J., Slip Velocity in Flow and Heat Transfer of Non-Newtonian Fluids in Microchannels, *International Journal of Engineering*, Vol. 30, No. 7, 2017, pp. 1054-1065.
- [47] Vajravelu K., Cannon J.R. and Rollins D., Analytical and Numerical Solutions of Nonlinear Differential Equations Arising in Non-Newtonian Fluid Flows, *Journal of Mathematical Analysis and Applications*, Vol. 250, 2000, pp. 204-221.
- [48] Zhang Z., Xie Y., Zhang D. and Xie G., Flow Characteristic and Heat Transfer for Non-Newtonian Nanofluid in Rectangular Microchannels with Teardrop Dimples/Protrusions, *Open Physics*, Vol. 15, No. 1, 2017, pp. 197-206.
- [49] Sarma R., Gaikwad H. and Mondal P.K., Effect of Conjugate Heat Transfer on Entropy Generation in Slip-Driven Microflow of Power Law Fluids, *Nanoscale and Microscale Thermophysical Engineering*, Vol. 21, No. 1, 2017, pp. 26-44.
- [50] Trebotich D., Chang W. and Liepmann D., Modeling of Blood Flow in Simple Microchannels, *Modeling and Simulation of Microsystems*, 2001, pp. 218-222.
- [51] Davidson P.A., *Magnetohydrodynamics in Materials Processing*, *Annual Reviews Fluid Mechanics*, Vol. 31, 1999, pp. 273-300.
- [52] Lemoff A.V., Lee A.P., Miles R.R. and McConaghy C.F., An AC Magnetohydrodynamic Micropump: Towards a True Integrated Microfluidic System, 10th International Conference on Solid-State Sensors and Actuators, Sendai, Japan, 1999.
- [53] Chaabane R., Bouras A and Nasrallah S.B., Numerical Magneto Hydro Dynamic Flow Simulation of Velocity and Pressure for Electrically Conducting, Incompressible Fluids,

- Journal of the Brazilian Society of Mechanical Sciences and Engineering , Vol. XXIX, No. 3, 2007, pp. 299-306.
- [54] Molokov S. and Reed C.B., Liquid Metal MHD Flows in Circular Ducts at Intermediate Hartmann Numbers and Interaction Parameters, *Magnetohydrodynamics*, Vol. 39, No. 4, 2003, pp. 539-546.
- [55] Öztürk A., MHD Slip Flow Between Parallel Plates Heated with a Constant Heat Flux, *Journal of Thermal Science and Technology*, Vol. 33, Issue 1, 2013, pp. 11-20.
- [56] Aoki L.P., Maunsell M.G. and Schulz H.E., A Magnetohydrodynamic Study of Behavior in an Electrolyte Fluid Using Numerical and Experimental Solutions, *Engenharia Térmica (Thermal Engineering)*, Vol. 11, No. 1-2, 2012, pp. 53-60.
- [57] National Research Council, *High Magnetic Field Science and Its Application in the United States: Current Status and Future Directions*. Washington, DC: The National Academies Press, 2013, pp. 5-103.
- [58] Kiyasatfar M., Pourmahmoud N., Golzan M. and Mirzaee I., Investigation of Thermal Behavior and Fluid Motion in Direct Current Magnetohydrodynamic Pumps, *Thermal Science*, Vol. 18, Suppl. 2, 2014, pp. S551-S562.
- [59] Khodak A., Numerical Analysis of 2-D and 3-D MHD Flows Relevant to Fusion Applications, *IEEE Transactions on Plasma Science*, vol. 45, no. 9, 2017, pp. 2561-2565.
- [60] Hasan M.I., Ali A.J.F. and Tufah R.S., Numerical Analysis of the Magnetohydrodynamic Flow and Heat Transfer in Microchannel, *International Journal of Computer Applications*, Vol. 149, No. 2, 2016, pp. 1-7.
- [61] Hasan M.I., Ali A.J.F. and Tufah R.S., Numerical study of the effect of channel geometry on the performance of Magnetohydrodynamic micro pump, *Engineering Science and Technology, an International Journal*, Vol. 20, Issue 3, 2017, pp. 982-989.
- [62] Rana A., Shit G.C. and Reza M., Patterned Hydrodynamic Slip Flow Control and Thermal Transport in a Wavy Microchannel through Porous Medium with Combined Electromagnetohydrodynamic Effect, *Journal of Physics: Conference Series*, Vol. 1849, 2021, pp. 1-9.
- [63] Krasnov D., Boeck T., Braiden L., Molokov S. and Bühler L., Numerical Simulations of MHD Flow Transition in Ducts with Conducting Hartmann Walls Limtech Project A3 D4 (TUI), KIT Scientific Publishing, 2016, pp. 1-21.
- [64] Gao C. and Jian Y., Analytical Solution of Magnetohydrodynamic Flow of Jeffrey Fluid Through a Circular Microchannel, *Journal of Molecular Liquids*, Vol. 211, 2015, pp. 803-811.

- [65] Oyekunle T.L., Akolade M.T., Agunbiade S.A. and Momoh H.O., Second-Order Slip Effect on the Flow of MHD Chemically Reacting Fluid Through an Inclined Micro-Annular Channel, *Mathematics and Computational Sciences*, Vol. 3, No. 3, 2022, pp. 11-28.
- [66] Oztop H.F., Al-Salem K. and Pop I., MHD Mixed Convection in a Lid-Driven Cavity with Corner Heater, *International Journal of Heat and Mass Transfer*, Vol. 54, 2011, pp. 3494-3504.
- [67] Sharma M.K., Singh K. and Kumar A., MHD Flow and Heat Transfer Through a Circular Cylinder Partially Filled with Non-Darcy Porous Media, *International Journal of Innovative Technology and Exploring Engineering*, Vol. 4, Issue 7, 2014, pp. 30-42.
- [68] Narayana K.L. and Gangadhar K., Second Order Slip Flow of a MHD Micropolar Fluid over an Unsteady Stretching Surface, *Advances in Applied Science Research*, Vol. 6, No. 8, pp. 224-241.
- [69] Rabbi K.Md., Saha S., Mojumder S., Rahman M.M., Saidur R. and Ibrahim T.A., *Alexandria Engineering Journal*, Vol. 55, 2016, pp. 127-139.
- [70] Shit G.C., Ranjit N. K. and Sinha A., Electro-magnetohydrodynamic Flow of Biofluid Induced by Peristaltic Wave: A Non-newtonian Model, *Journal of Bionic Engineering*, Vol. 13, 2016, pp. 436-448.
- [71] Sharma M.K., Singh K. and Kumar A., MHD Flow and Heat Transfer Through a Circular Annulus of Non-Darcy Porous Media Saturated with Viscous Incompressible Fluid, *International Journal of Recent Scientific Research*, Vol. 9, Issue 10(C), 2018, pp. 29222-29228.
- [72] Nagaraju G., Garvandha M. and Murthy J.V.R., MHD Flow in a Circular Horizontal Pipe under Heat Source/Sink with Suction/Injection on Wall, *Frontiers in Heat and Mass Transfer*, Vol. 13, Issue 6, 2019, pp. 1-8.
- [73] Tulu A. and Ibrahim W., MHD Slip Flow of CNT-Ethylene Glycol Nanofluid due to a Stretchable Rotating Disk with Cattaneo–Christov Heat Flux Model, *Mathematical Problems in Engineering*, Vol. 2020, 2020, pp. 1-13.
- [74] Sheikholeslami M. and Farshad S.A., Investigation of Solar Collector System with Turbulator Considering Hybrid Nanoparticles, *Renewable Energy*, Vol. 171, 2021, pp. 1128-1158.
- [75] Buren M., jian Y., Chang L., Liu Q. and Zhao G., AC Magnetohydrodynamic Slip Flow in Microchannel with Sinusoidal Roughness, *Microsyst Technol*, Vol. 23, 2017, pp. 3347-3359.

- [76] Kiyasatfar M. and Pourmahmoud N., Laminar MHD Flow and Heat Transfer of Power-Law Fluids in Square Microchannels, *International Journal of Thermal Sciences*, Vol. 99, 2016, pp. 26-35.
- [77] Reddy M.G., Velocity and Thermal Slip Effects on MHD Third Order Blood Flow in an Irregular Channel Through a Porous Medium with Homogeneous/Heterogeneous Reactions, *Nonlinear Engineering*, Vol. 6, Issue 3, 2017, pp. 167-177.
- [78] Sushma S., Samuel N. and Neeraja G., Slip Flow Effects on Unsteady MHD Blood Flow in a Permeable Vessel in the Presence of Heat Source/Sink and Chemical Reaction, *Global Journal of Pure and Applied Mathematics*, Vol. 14, No. 8, 2018, pp. 1083-1099.
- [79] Andreev O., Kolesnikov Yu. and Thess A., Experimental Study of Liquid Metal Channel Flow under the Influence of a Nonuniform Magnetic Field, *Physics of Fluids*, Vol. 18, 2006, pp. 065108/1-11.
- [80] Ghasemi B., Aminossadati S.M. and Raisi A., Magnetic Field Effect on Natural Convection in a Nanofluid-Filled Square Enclosure, *International Journal of Thermal Sciences*, Vol. 50, 2011, pp. 1748-1756.
- [81] Hoseinzadeh S., Heyns P.S. and Kariman H., Numerical Investigation of Heat Transfer of Laminar and Turbulent Pulsating  $\text{Al}_2\text{O}_3$ /Water Nanofluid Flow, *International Journal of Numerical Methods for Heat & Fluid Flow*, Vol. 30, No. 3, 2020, pp. 1149-1166.
- [82] Lalami A.A., Afrouzi H.H. and Moshfegh A., Investigation of MHD Effect on Nanofluid Heat Transfer in Microchannels: An incompressible lattice Boltzmann approach, *Journal of Thermal Analysis and Calorimetry*, Vol. 30, 2019, pp. 1959-1975.
- [83] Sheikholeslami M., Gorji-Bandpy M. and Ganji D.D., Numerical Investigation of MHD Effects on  $\text{Al}_2\text{O}_3$ -Water Nanofluid Flow and Heat Transfer in a Semi-Annulus Enclosure using LBM, *Energy*, Vol. 60, 2013, pp. 501-510.
- [84] Escandón J.P., Bautista O.E., Santiago F. and Méndez F., Asymptotic Analysis of Non-Newtonian Fluid Flow in a Microchannel Under a Combination of EO and MHD Micropumps, *Defect and Diffusion Forum*, Vol. 348, 2014, pp. 147-152.
- [85] Das S., Jana R.N. and Makinde O.D., MHD Boundary Layer Slip Flow and Heat Transfer of Nanofluid Past a Vertical Stretching Sheet with Non-Uniform Heat Generation/Absorption, *International Journal of Nanoscience*, Vol. 13, No. 3, 2014, pp. 1450019/1-12.
- [86] Elelamy A.F., Elgazery N.S. and Ellahi R., Blood Flow of MHD Non-Newtonian Nanofluid with Heat Transfer and Slip Effects: Application of Bacterial Growth in Heart Valve, *International Journal of Numerical Methods for Heat & Fluid Flow*, Vol. 30, No. 11, 2020, pp. 4883-4908.

- [87] Arjun K.S. and Rakesh K., Heat Transfer Enhancement using Alumina Nanofluid in Circular Micro Channel, *Journal of Engineering Science and Technology*, Vol. 12, No. 1, 2017, pp. 265-279.
- [88] Arani A.A.A., Sheikhzadeh G.A. and Arani A.G., Study of Fluid Flow and Heat Transfer of AL<sub>2</sub>O<sub>3</sub>-Water as a Non-Newtonian Nanofluid through Lid-Driven Enclosure, *Transport Phenomena in Nano-Micro Scale*, Vol. 2, 2014, pp. 118-131.
- [89] Sheikholeslami M., Hayat T. and Alsaedi A., MHD Free Convection of Al<sub>2</sub>O<sub>3</sub>-Water Nanofluid Considering Thermal Radiation: A Numerical Study, *International Journal of Heat and Mass Transfer*, Vol. 96, 2016, pp. 513-524.
- [90] Raja Sekhar Y. and Sharma K.V., Study of Viscosity and Specific Heat Capacity Characteristics of Water-Based Al<sub>2</sub>O<sub>3</sub> Nanofluids at Low Particle Concentrations, *Journal of Experimental Nanoscience*, Vol. 10, No. 2, 2015, pp. 86-102.
- [91] Karimipour A., D’Orazio A. and Shadloo M.S., The effects of different nano particles of Al<sub>2</sub>O<sub>3</sub> and Ag on the MHD nano fluid flow and heat transfer in a microchannel including slip velocity and temperature jump, *Physica E: Low-dimensional Systems and Nanostructures*, Vol.86, 2017, pp.146-153.
- [92] Kumar R., Raju C. S. K., Sekhar K. R. and Reddy G. V., Three dimensional MHD ferrous nanofluid flow over a sheet of variable thickness in slip flow regime, *Journal of Mechanics*, Vol.35, No.2, 2019, pp. 255-266.
- [93] Das S., Jana R.N., Makinde O. D., MHD Flow of Cu-Al<sub>2</sub>O<sub>3</sub>/Water Hybrid Nanofluid in Porous Channel: Analysis of Entropy Generation, *Defect and Diffusion Forum*, vol.377, September, 2017, pp.42-61.
- [94] Gangadhar K., Bhargavi D.N., Kannan T., Rao M.V. S. and Chamkha A.J., Transverse MHD flow of Al<sub>2</sub>O<sub>3</sub>-Cu/H<sub>2</sub>O hybrid nanofluid with active radiation: A novel hybrid model, *Math Meth Appl Sci*, May, 2020, pp. 1-19.
- [95] Ghalambaz M., Mehryan S. A. M., Izadpanahi E., Chamkha A. J., and Wen D., MHD natural convection of Cu-Al<sub>2</sub>O<sub>3</sub> water hybrid nanofluids in a cavity equally divided into two parts by a vertical flexible partition membrane, *Journal of Thermal Analysis and Calorimetry*, May 2019, pp. 1-21.
- [96] Iftikhar N., Rehman A., Sadaf H., and Iqbal S., Study of (Al<sub>2</sub>O<sub>3</sub> & copper)/ water nanoparticles shape, slip effects and heat transfer on steady physiological delivery of MHD hybrid nanofluid, *Canadian Journal of Physics*, vol. 97, no.12, December 2019, pp. 1-35.
- [97] Jain S., Bhargava R., Numerical simulation of free convection of MHD non-Newtonian nanofluid within a square wavy enclosure using Mesh free method, *International Journal for Computational Methods in Engineering Science and Mechanics*, Nov 2020, pp. 1-13.

- [98] Qomi M.E, Sheikhzadeh G.A. and Fattahi A., Heat transfer enhancement in a microchannel using a pulsating MHD hybrid nanofluid flow, Energy Sources, Part A: Recovery, Utilization, and Environmental Effects, 2020, pp. 1-17.
- [99] Brinkman H.C., The viscosity of concentrated suspensions and solution, The Journal of Chemical Physics, vol. 20, no.4, April 1952, pp. 571-581.
- [100] Bazinet L, Trigui M. and Ippersiel D., Rheological Behaviour of WPI dispersion as a function of pH and protein concentration. Journal of Agricultural and Food Chemistry, vol. 52, 2004, pp. 5366-5371.
- [101] Elblbesy M. A. and Hereba A. T., Computation of the Coefficients of the Power law model for Whole Blood and Their Correlation with Blood Parameters, Applied Physics Research; Vol. 8, No. 2; 2016 pp. 1-9.
- [102] Shekarforoush E., Faralli A., Ndoni S, Mendes A.C. and Chronakis I.S. Electrospinning of Xanthan polysaccharide. Macromolecular Materials and Engineering, vol. 302, 2017,pp. 1700067 (1 to 11).

*Sahyabir Babbar*  
15/12/2022